Alkane Dehydrogenation and H/D Exchange by a Cationic Pincer-Ir(III) Hydride: A Novel Mechanism of C-H Addition and β -H Elimination Leads to Unprecedented Selectivity

Ashish Parihar^a, Thomas J. Emge^a, Faraj Hasanayn^{b*}, Alan S. Goldman^{a*}

Abstract

We report that the cationic iridium complex (iPrPCP)IrH+ undergoes addition of alkane C-H bonds, which is manifested by catalytic alkane transfer-dehydrogenation to give alkenes and by hydrogen isotope (H/D) exchange (HIE). Contrary to established selectivity trends found for C-H activation by transition metal complexes, strained cycloalkanes, including cyclopentane, cycloheptane, and cyclooctane, undergo C-H addition much more readily than n-alkanes which in turn are much more reactive than cyclohexane. Aromatic C-H bonds also undergo H/D exchange much less rapidly than those of the strained cycloalkanes, but much more favorably than cyclohexane. The order of reactivity toward dehydrogenation correlates qualitatively with the reaction thermodynamics, but the magnitude is much greater than can be explained by thermodynamics. Accordingly, the cycloalkenes corresponding to the strained cycloalkanes undergo hydrogenation much more readily than cyclohexene, despite the less favorable thermodynamics of such hydrogenations. Computational (DFT) studies allow rationalization of the origin of reactivity and the unusual selectivity. Specifically, the initial C-H addition is strongly assisted by β -agostic interactions, which are particularly favorable for the strained cycloalkanes. Subsequent to α -C-H addition, the H atom of the β -agostic C-H bond is transferred to the hydride ligand of (iPrPCP)IrH+, to give a dihydrogen ligand. The overall processes, C-H addition and β-H-transfer to hydride, generally show intermediates on the IRC surface but they are extremely shallow, such that the 1,2-dehydrogenations are presumed to be effectively concerted although asynchronous.

^a Department of Chemistry and Chemical Biology, Rutgers, The State University of New Jersey, New Brunswick, New Jersey 08903, United States

^b Department of Chemistry, American University of Beirut, Beirut 1107 2020, Lebanon

^{*}Email: fh19@aub.edu.lb; alan.goldman@rutgers.edu

■ INTRODUCTION

Iridium has played a prominent role in the chemistry of C-H activation and functionalization, largely through C-H activation by low oxidation state (specifically, Ir^I) centers,¹⁻⁵ although examples of C-H activation by high-valent complexes have long been known as well.⁶⁻⁹ With respect to catalysis, alkane dehydrogenation by pincer-ligated low-valent iridium complexes has been particularly well studied.¹⁰⁻¹¹ In the past decade, however, there has been significant progress in the development of pincer-iridium-based catalysts believed to operate entirely via high-valent oxidation states.¹²⁻¹⁶ Recently, we reported that the (*p*-pyridyl-^{tBu}PCP)IrCl+ cation (*p*-pyridyl-^{tBu}PCP = 3,5-bis(di-tert-butylphosphinomethyl)-2,6-dimethylpyridin-4-yl) undergoes facile *intramolecular* C(sp³)-H activation¹⁷. We computationally investigated C-H activation by the parent Ir^{III} complex (^{tBu}PCP)IrCl+ (^RPCP = 2,6-C₆H₃(CH₂PR₂)) and the less crowded analog (^{IP}PCP)IrCl+. DFT calculations indicated that (^{IP}PCP)IrCl+ would more favorably undergo intermolecular rather than intramolecular C-H activation (Scheme 1). Moreover, intermolecular C-H addition of alkanes by this fragment was predicted to lead to dehydrogenation to yield olefins.¹⁷

Scheme 1. Relative free energies for cyclometalation (intramolecular sp³ C-H activation) versus intermolecular sp³ C-H activation (propane used as model alkane; from reference 17).

High-valent systems for dehydrogenation of alkanes or alkyl groups hold the intriguing possibility that they might tolerate functional groups or reagents not compatible with low-valent systems, or that they may offer selectivity complementary to low-valent systems. In consideration of these points, we attempted to pursue an experimental investigation of the predicted catalytically active fragment (^{iPr}PCP)IrCl⁺. While we were unsuccessful in this effort, we found that the isoelectronic fragment (^{iPr}PCP)IrH⁺ is an active catalyst for alkane dehydrogenation and H/D exchange. Interestingly, it shows selectivity that is dramatically

different from that of low-valent species (most notably, (iPrPCP)Ir and related fragments). Calculations indicate this selectivity can be rationalized based on a novel pathway, one which is very distinct from pathways reported for low-valent (RPCP)Ir-based catalysts and widely assumed to be operative for dehydrogenation catalysts based on transition metals in low oxidation states more generally.

■ EXPERIMENTAL RESULTS

Synthesis of (^{iPr}**PCP)IrH**⁺. Motivated by the experimental and computational studies noted above, we attempted to synthesize (^{iPr}PCP)IrCl⁺ via the reaction of (^{iPr}PCP)IrHCl (**1-HCl**) with [H(Et₂O)₂][BArF²⁴]¹⁹ (Scheme 2), as well as with H[PF₆] and HCl²⁰. These efforts, however, were unsuccessful.

Scheme 2. Attempted generation of (iPrPCP)IrCl+ by reaction of **1-HCl** with [H(Et₂O)₂][BArF²⁴].

Scheme 3. Generation of [1-H⁺][BArFⁿ] by reaction of 1-HCl with M[BArFⁿ].

We therefore considered investigation of the isoelectronic fragment (^{iPr}PCP)IrH+ (**1-H**+), an analog of ($^{tBu}POCOP$)IrH+ ($^{tBu}POCOP = 2,6-C_6H_3(OP^tBu_2)_2$), the chemistry of which has been extensively developed by Brookhart and co-workers. $^{21-27}$ Toward this end **1-HCI** was treated with M[BArF²⁰] or M[BArF²⁴] (M = Na, Li, K; BArF²⁰ = B(C₆F₅)₄; BArF²⁴ = B[3,5-C₆H₃(CF₃)₂)]₄; Scheme 3). The room-temperature $^{31}P[^{1}H]$ NMR spectrum of a light orange toluene- d 8 solution resulting from the reaction with Na[BArF²⁴] predominantly featured a very broad peak at δ 55

with several minor sharp peaks at δ 36 to δ 55. At 100 °C, however, the ³¹P[¹H] NMR spectrum showed only a single fairly sharp peak at δ 59.7. The ¹H NMR spectrum at 100 °C showed only one, fairly broad, peak upfield of δ 0 (i.e. the hydride region), specifically at δ -41.59, integrating as 1 H relative to the characteristic pincer-ligand and BArF²⁴ signals, indicative of a hydride ligand positioned trans to a vacant coordination site²⁸. When the temperature was lowered this peak broadened further and at room temperature it was not observable, nor were any other signals seen in the upfield region. We attribute these observations to the presence of only one species in solution at 100 °C, best described as (^{iPr}PCP)IrH+ (1-H+), although weak and dynamic interactions with solvent, anion, or other species in solution seem likely. At room temperature, such interactions, perhaps including the binding of solvent impurities, are presumably less dynamic.

(^{iPr}PCP)IrH⁺: addition of small molecules and further characterization. When CO atmosphere was added to a dichloromethane solution of [1-H⁺][BArF²⁴] followed by removal of solvent and dissolution in CDCl₃, the ³¹P[¹H] NMR spectrum showed a single sharp signal at δ 51.11, while a signal at δ -10.42 (t, ³J_{PH} = 12.8 Hz) was found in the ¹H NMR spectrum, suggestive of the formation of [1-H(CO)₂+][BArF²⁴] (Scheme 4). Crystals were obtained by vapor diffusion of pentane into a benzene solution and scXRD confirmed characterization as [*cis*-1-H(CO)₂+][BArF²⁴] (Figure 1).

Scheme 4. Reaction of **1-HCl** with Na[BArF²⁴] to generate putative **1-H**⁺ under CO atmosphere leading to **1-H(CO)**₂⁺.

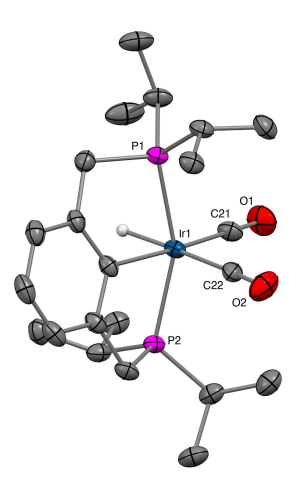


Figure 1. Molecular structure of [*cis*-(^{iPr}PCP)IrH(CO)₂] cation determined by scXRD. Hydrogen atoms, except for the hydride ligand, and BArF²⁴ anion omitted for clarity.

Addition of H_2 atmosphere to a toluene- d^8 solution of **1-H**⁺ resulted in the formation of two signals in the $^{31}P[^1H]$ NMR spectrum at approximately δ 55 and δ 57 ppm in a ratio of ca 70:30. In the 1H NMR spectrum (toluene- d_8), two peaks in the metal-hydride region were observed at approximately δ -3.99 ppm and δ -26.88, in a ratio of 2:1, consistent with an assignment of $[(^{iPr}PCP)IrH(H_2)][BArF^{24}]$ ([**1-H(H₂)**][BArF²⁴]); the $^{tBu}POCOP$ analog of this species has been reported by Brookhart and co-workers²⁶. HMBC spectroscopy revealed that the hydride signals correlated with the major signal in the $^{31}P[^1H]$ NMR spectrum.

Propene, *t*-butylethylene (TBE), and cyclopentene (CPE) were added to separate toluene-d₈ solutions of [**1-H**⁺][BArF²⁴]. In all three cases an upfield signal was observed in the ¹H NMR spectrum (-34.2 ppm, -30.7 ppm, and -33.4 ppm, respectively), indicative of an olefin complex with a hydride ligand positioned trans to a vacant coordination site, and therefore presumably **1-H(alkene)**⁺. In the cases of TBE and CPE the ¹H NMR signals due to the free olefin in solution were broad, indicating exchange between free and coordinated olefin (signals attributable to coordinated olefin were not observed). With propene, the free olefin signal was sharp at room temperature but broadened at higher temperature, ca. 320 K. A single peak was observed in the ³¹P NMR spectrum with each alkene: propene, 46.3 ppm; TBE, 51.2 ppm (broad); CPE, 38.8 ppm. (Details are found in the Supporting Information.)

When 1 atmosphere ethylene was added to a toluene-d₈ solution of [1-H⁺][BArF²⁴], at room temperature the ¹H NMR signal attributable to free ethylene was very broad, at 5.1 ppm (cf.

5.25 ppm in the absence of metal complex³⁹). In the ³¹P[¹H] NMR spectrum an extremely broad signal is observed at 29.6 ppm. No hydride signal was observed at room temperature but at 233 K a signal appears at -13.3 ppm, attributable, in contrast to the complexes discussed above, to a hydride positioned trans to a strong trans-influence ligand. At this temperature, the free ethylene signal in the ¹H NMR spectrum was relatively sharp, at 5.24 ppm. In the ³¹P[¹H] NMR spectrum an extremely broad signal is observed at 29.6 ppm at room temperature, while at 233K a relatively sharp signal is found at 27.18 ppm. Under 1.6 atm ethylene, the signal in the room-temperature ³¹P[¹H] NMR spectrum was sharper than observed under 1.0 atm, and shifted to 28.6 ppm. These results are all consistent with rapid exchange between coordinated and free ethylene, and an equilibrium between the mono- and bis-ethylene complexes, $1-H(C_2H_4)^+$ and $1-H(C_2H_4)_2^+$.

Thus, ethylene, propene, CPE, and TBE are all found to bind to **1-H**⁺ and to undergo exchange between free and coordinated alkene on the NMR timescale. Only in the case of the least sterically demanding alkene, ethylene, is there evidence for a significant equilibrium concentration of bis-ethylene complex, and this is apparently the major species in solution at 233 K.

Alkane dehydrogenation by 1-H⁺: initial screenings. The addition of Li[BArF²⁰] to cyclooctane (COA) solutions containing TBE and 1-HCl was found to result in high rates of catalytic COA-to-TBE transfer dehydrogenation (Figure 2a). No dehydrogenation was observed under the same conditions when no alkali metal salt was added to the 1-HCl. Addition of 3 equiv Li[BArF²⁰] gave somewhat greater activity than with 1 equiv Li[BArF²⁰], but the use of 6 equiv Li[BArF²⁰] gave no more activity than with 3 equiv; this seems consistent with incomplete halide removal by 1 equiv, and essentially complete removal with the use of 3 equiv.

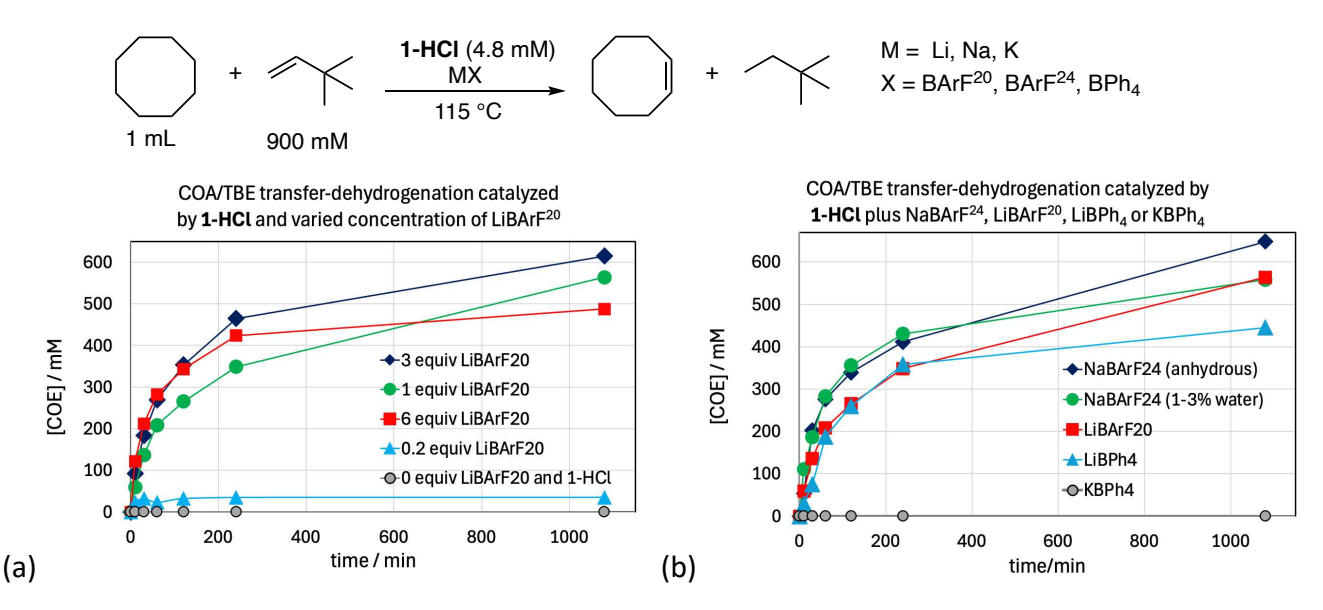


Figure 2. (a) COA/TBE transfer-dehydrogenation catalyzed by **1-HCl** and various quantities of Li[BArF²⁰] (b) COA/TBE transfer-dehydrogenation catalyzed by **1-HCl** and Li[BPh₄], Na[BArF²⁴] or KBPh₄.

Salts of Li⁺, Na⁺, K⁺ were investigated, with non-coordinating anions including BPh₄, BArF²⁰, and BArF²⁴. No dehydrogenation was obtained with K[BPh₄] presumably due to very poor solubility. 1.0 equiv Na[BArF²⁴] (either anhydrous or 1-3% H2O) afforded a level of catalytic activity very comparable to 3 equiv Li[BArF²⁰]. Additional Na[BArF²⁴] had no significant effect. These results suggest that chloride was fully removed with the use of 1.0 equiv Na[BArF²⁴]. Subsequently, for purposes described below, unless indicated otherwise, 1-H⁺ was prepared *in situ* by the reaction of 1-HCl with Na[BArF²⁴] at 115 °C.

Several hydrogen acceptors were investigated for COA transfer-dehydrogenation. 1-hexene and t-butylpropene (TBPE; 4,4-dimethylpent-1-ene) were found to undergo rapid isomerization to form internal olefins, affording low rates and turnover numbers (TONs) for transfer-dehydrogenation²⁹⁻³⁰ (Figure 3a). TBE proved significantly more effective than other acceptors and was used as the standard acceptor for further transfer-dehydrogenation experiments in this study.

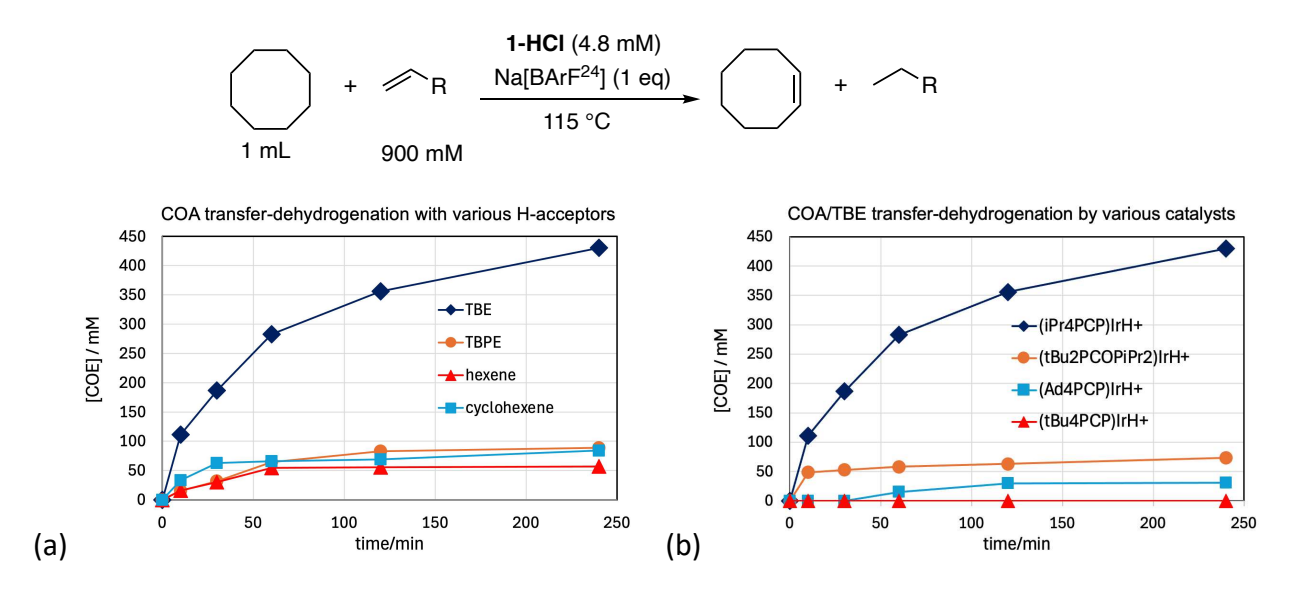


Figure 3. (a) COA transfer-dehydrogenation by **1-H**⁺ with use of various hydrogen acceptors. (b) COA/TBE transfer-dehydrogenation by various complexes (pincer)IrHCl and MX (presumed to generate the corresponding species (pincer)IrH⁺).

Iridium complexes of other PCP-type pincer ligands were investigated for catalytic activity under the same conditions as described above (Figure 3b). The archetypal (tBu PCP)IrHCl gave no observable COA/TBE transfer-dehydrogenation activity; the contrast with **1-HCl** is particularly striking considering that the corresponding (tBu PCP)Irl fragment is generally highly effective for transfer-dehydrogenation (albeit less so than (iPr PCP)Irl)²⁹. This may be attributable to purely steric factors; we have calculated¹⁷ in the case of (R PCP)IrCl+ that intermolecular C-H bond addition (a terminal C-H bond of propane) has a barrier, ΔG^{\ddagger} , 7.5 kcal/mol higher for tBu PCP than for iPr PCP. Alternatively, the negligible activity of (tBu PCP)IrHCl may be attributable to cyclometalation; both kinetically ($\Delta \Delta G^{\ddagger}$ = -2.0 kcal/mol), and thermodynamically ($\Delta \Delta G^{\circ}$ = -4.7 kcal/mol), (tBu PCP)IrCl+ is calculated to be much more prone to cyclometalation than (iPr PCP)IrCl+.¹⁷

The tetra-adamantyl substituted complex (AdPCP)IrHCl showed activity slightly higher than (tBuPCP)IrHCl, but still much less than (iPrPCP)IrHCl; the increase vis-à-vis (tBuPCP)IrHCl may be due to AdPCP being slightly less sterically demanding, or its greater resistance to cyclometallation (Figure 3b). The mixed di-t-butylphosphino/di-i-propylphosphino complex (tBu2PCOPiPr2)IrHCl, was found to be more active than (AdPCP)IrHCl or (tBuPCP)IrHCl, but still much

less so than (iPrPCP)IrHCl. Accordingly, all further work in this study utilized only the iPrPCP pincer ligand.

Chemoselectivity of dehydrogenation: comparison between (PCP)Ir^{II} and (PCP)Ir^{III}H⁺.

Precursors of (pincer)Ir^I, including (^{IPr}PCP)Ir^I, are among the most effective and well known catalysts for alkane dehydrogenation, typically operating via an Ir^I/Ir^{III} cycle^{11, 32-33}. Given that the present and previously reported systems share the same (^{IPr}PCP)Ir unit, we felt it was critical to consider and investigate the possibility that the two systems operated via the same catalytically active species (even though there were no obvious bases or reductants present in the above-described examples of catalysis achieved with Ir^{III} precursors). To this end, we conducted selectivity competition experiments with sources of (^{IPr}PCP)Ir^{II} and with the putative fragment (^{IPr}PCP)Ir^{III}H⁺. These experiments not only demonstrated that the systems operated via different catalytically active species, they also revealed remarkable and unexpected differences in selectivity.

Addition of KO^tBu to **1-HCl** is known to generate the active species (^{iPr}PCP)Ir¹, ³⁴⁻³⁵ while the addition of Li[BArF²⁰] is presumed, based on the experiments described above, to generate (^{iPr}PCP)IrH⁺. Experiments were conducted in which a competition for dehydrogenation of COA versus *n*-decane was established, using TBE as H-acceptor, with **1-HCl** and one equiv of either KO^tBu or LiBArF²⁰. In the case of KO^tBu addition, greater activity, by a factor of ca. 2 on a per mol basis, was observed for the dehydrogenation of *n*-decane versus COA (Figure 4a). In contrast, the use of LiBArF²⁰ resulted in *much* greater (>200-fold) activity toward COA relative to *n*-decane (Figure 4b). These strongly contrasting selectivities support the conclusion of fundamental differences in the respective catalytic cycles of these two systems.

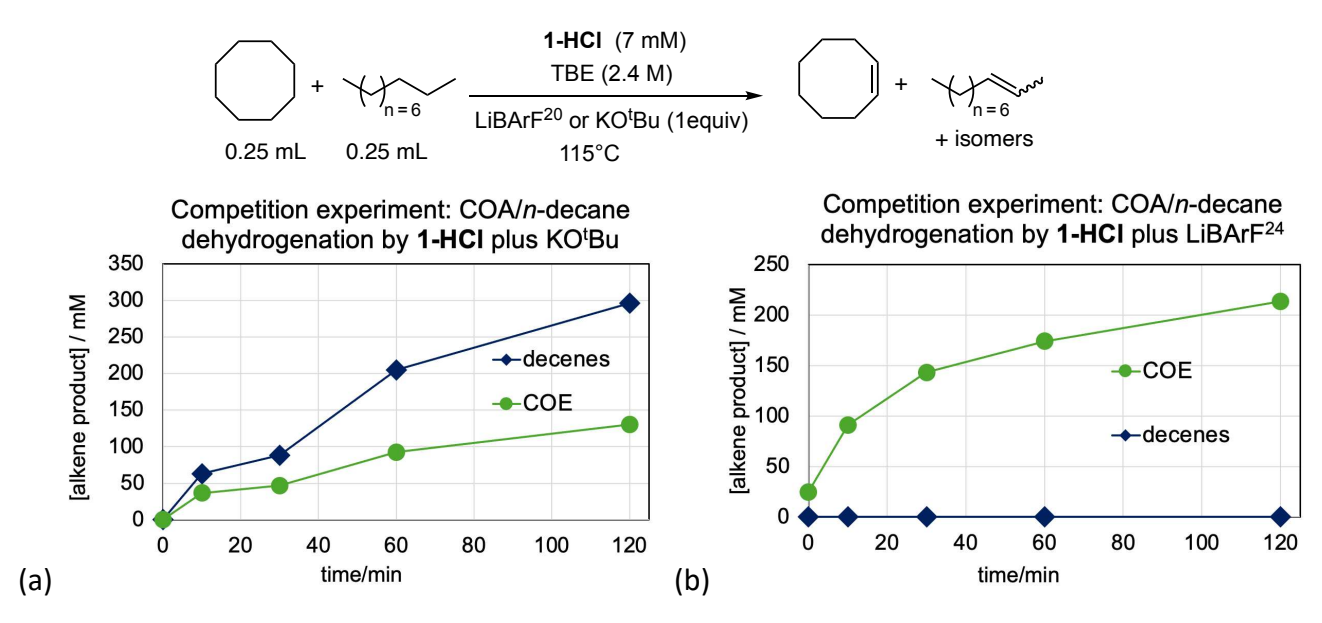


Figure 4. Competition experiments: transfer dehydrogenation of COA versus *n*-decane by (a) **1-HCl** and KO^tBu (presumably generating (^{iPr}PCP)Ir^l), and (b) by **1-HCl** and Li[BArF²⁰] (presumably generating (PCP)IrH⁺).

The same competition was conducted but catalyzed by (^{iPr}PCP)Ir(ethylene) and [H(Et₂O)₂][BArF²⁴]. The results were effectively the same as obtained with (^{iPr}PCP)IrHCl and Na[BArF²⁴], indicating a common, catalytically active fragment, presumably (^{iPr}PCP)IrH⁺.

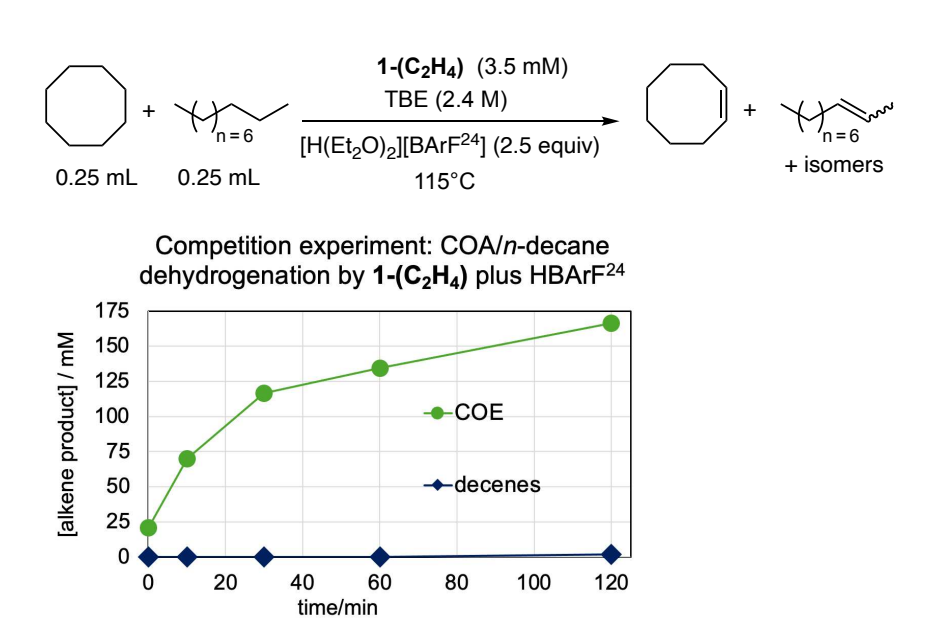


Figure 5. Competition experiment, transfer-dehydrogenation of COA versus n-decane catalyzed by (^{iPr}PCP)Ir(ethylene) and [H(Et₂O)₂][BArF²⁴] (cf. Figure 4b).

Further transfer-dehydrogenation competition experiments using 1-H⁺. Intrigued by the remarkably high selectivity for dehydrogenation of COA versus an *n*-alkane, we investigated the competition of other cycloalkanes with *n*-decane. We note that the results of competition experiments are determined solely by energy differences between the rate-determining TSs for different substrates.³⁶ In contrast, the rates of individual experiments are also controlled by relative resting state energies, which likely vary depending upon the binding energies of the respective alkene product, and may be further complicated by many factors such as allyl or diene formation as well as any impurities present in the substrate sources.

1-H⁺ (generated by the reaction of **1-HCl** with Na[BArF²⁴]) showed high selectivity for dehydrogenation of cyclopentane (CPA) versus n-decane, as was observed for COA versus n-decane, although "only" by a factor of ca. 13 (Figure 6a). Cyclododecane (CDA), however, was found to be much *less* reactive than n-decane (by a factor of ca. 20; Figure 6b). Thus the relative activity of the cycloalkanes (values relative to n-decane) is as follows: COA (>100:1) > CPA (ca. 10:1) > CDA (ca. 0.05:1). This order correlates with ring-strain in the respective cycloalkanes (Table 1): COA (9.6 kcal/mol) > CPA (6.5 kcal/mol) > CDA (4.8 kcal/mol).

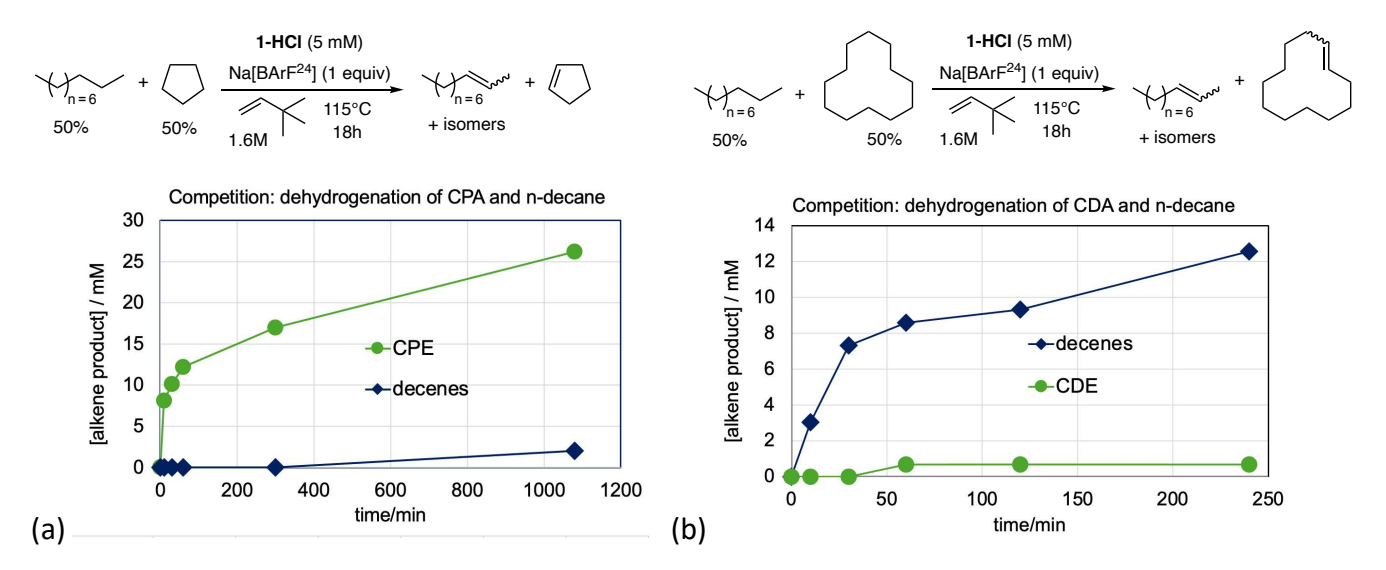


Figure 6. Transfer dehydrogenation catalyzed by **1-H** $^+$ with TBE as hydrogen acceptor. Competition experiment of (a) cyclopentane (CPA) versus n-decane and (b) cyclododecane (CDA) versus n-decane.

Table 1. Ring strain and dehydrog	enation enthalpies	of relevant alkanes
-----------------------------------	--------------------	---------------------

Dehydrogenation	Ring strain	Ring strain/CH ₂	Dehydrogenation
product	(cycloalkane)	(cycloalkane)	enthalpy (vs. C ₆ H ₁₂)
cyclopentene (CPE)	6.5	1.3	-1.2
cyclohexene (CHxE)	0.0	0.0	0.0
cycloheptene (CHpE)	6.3	0.9	-2.0
cyclooctene (COE)	9.6	1.2	-3.5
cyclododecene (CDE)	4.8	0.4	-1.7
1-decene			+2.0
trans-2-decene			-0.2
TBE			+2.1

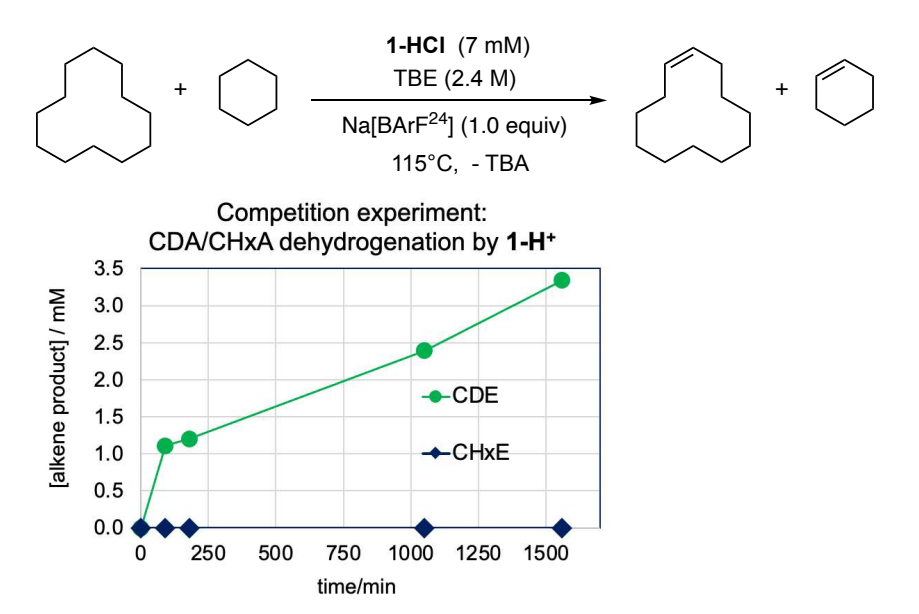


Figure 7. Transfer dehydrogenation catalyzed by **1-H**⁺ with TBE as hydrogen acceptor. Competition experiment of cyclododecane (CDA) versus cyclohexane (CHxA).

Thus CDA was found to be far less reactive than *n*-alkanes toward dehydrogenation by **1-H**⁺, and *n*-alkanes in turn far less reactive than COA or CPA. Nevertheless, cyclohexane (CHxA) was found to be even much less reactive than CDA (Figure 7). Indeed, no cyclohexene was observed in a CDA/CHxA dehydrogenation competition experiment; thus the ratio could not be quantified but the extremely low level of susceptibility of CHxA toward dehydrogenation by **1-H**⁺ can clearly be inferred.

Hydrogenation by (PCP)IrH⁺. A correlation of dehydrogenation reactivity with ring strain among cycloalkanes is not in itself surprising. Ring strain in medium-sized rings generally

correlates with thermodynamics of dehydrogenation (Table 1 shows ring strain and dehydrogenation enthalpies), and the dehydrogenation thermodynamics will in turn correlate with rates if the rate-determining transition state has some cycloalkene character. However, we found the large magnitude of the dehydrogenation selectivity to be surprising.

While the very high reactivities of COA and CPA relative to *n*-decane are consistent with their lower enthalpy (lesser endothermicity) of dehydrogenation, the very low relative reactivity of CDA does not seem to correlate with its dehydrogenation enthalpy. (The dehydrogenation enthalpy of CDA is slightly more negative than that of CPA, for example, and significantly more negative than that of *n*-decane to give either terminal or internal olefins; Table 1). In order to further investigate the relative reactivity of these substrates we studied the reverse reaction, hydrogenation of the corresponding olefins.

Hydrogenation (with H_2) is not the microscopic reverse of transfer-dehydrogenation. Nevertheless, if the rate-determining step follows addition of olefin and net addition of 2 H to the metal center in pathways for both transfer-hydrogenation and for hydrogenation using H₂, the selectivity in competition experiments should be the same regardless of the hydrogen source. In accord with this point, the very high reactivity of (iPrPCP)IrH+ for the dehydrogenation of COA versus linear alkane was also reflected in hydrogenation competition experiments. Competition experiments between hydrogenation of COE versus TBE were performed using (iPrPCP)Irl and using (iPrPCP)Irll H⁺. The rapid rate of the hydrogenation reaction, with either catalyst, precluded direct observation of kinetics. Instead, hydrogen gas (H₂) was incrementally added to the reaction vessel and concentrations were determined by ¹H NMR spectroscopy, allowing the determination of relative rates. When catalyzed by (PCP)Ir^I (1-HCI/KO^tBu) hydrogenation was essentially completely selective for TBE, with negligible COE hydrogenation detected (Figure 8a), consistent with the much more favorable thermodynamics of TBE hydrogenation. However, when catalyzed by 1-H⁺ (1-HCI/NaBArF²⁴), hydrogenation of COE and TBE proceeded at virtually identical rates (Figure 8b), highlighting the point that the Irl and Irll catalysts operate through very different mechanisms and, in particular, the far greater relative effectiveness of the IrH⁺ system for COA/COE dehydrogenation/hydrogenation.

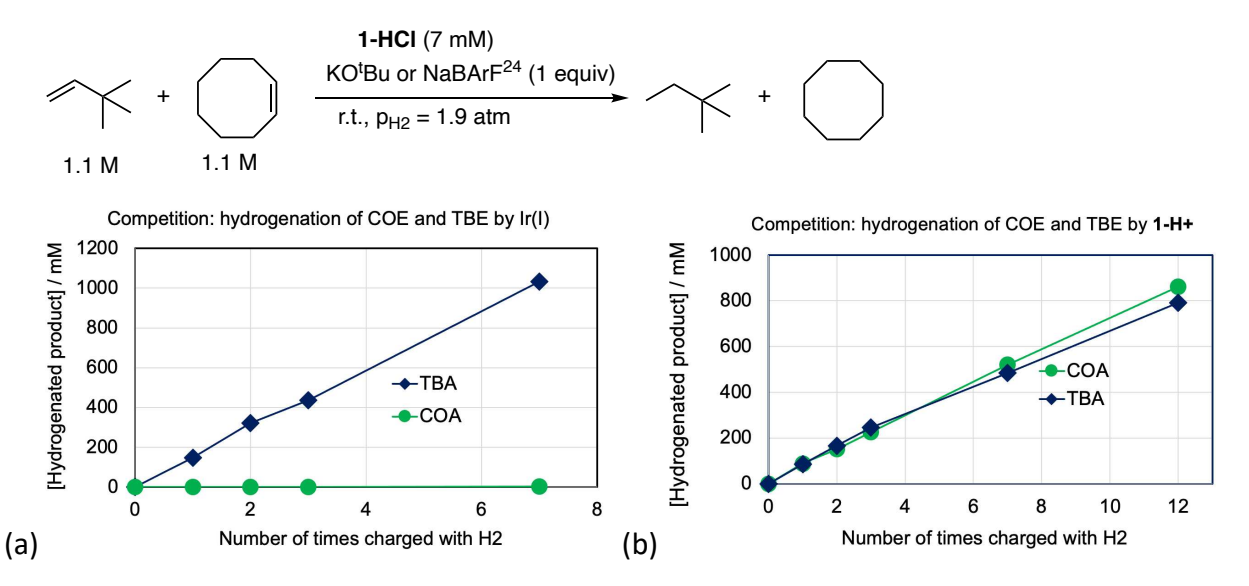


Figure 8. (a) Competition hydrogenation experiments: (a) COE versus TBE catalyzed by (^{iPr}PCP)Ir(I) (b) COE versus TBE hydrogenation catalyzed by (^{iPr}PCP)IrH⁺

The reaction enthalpy of TBE hydrogenation is 5.6 kcal/mol more negative than that of COE hydrogenation (Table 1). Given that, and considering that COE is a disubstituted olefin while TBE is monosubstituted, the extremely high selectivity for hydrogenation of TBE shown by (iPrPCP)Irl is not surprising. Rather, the approximately equal barriers for hydrogenation of COE and TBE when catalyzed by 1-H⁺ is very noteworthy.

The reaction enthalpy of hydrogenation of CPE is 2.3 kcal/mol more favorable than for COE hydrogenation, but still 3.3 kcal/mol less favorable than for TBE hydrogenation (Table 2). Nevertheless, in a competition experiment, CPE was hydrogenated more rapidly than TBE (Figure 9a). Likewise, CHpE has a hydrogenation enthalpy 4.1 kcal/mol less negative than TBE, but is hydrogenated ca. 4x more rapidly (Figure 9b).

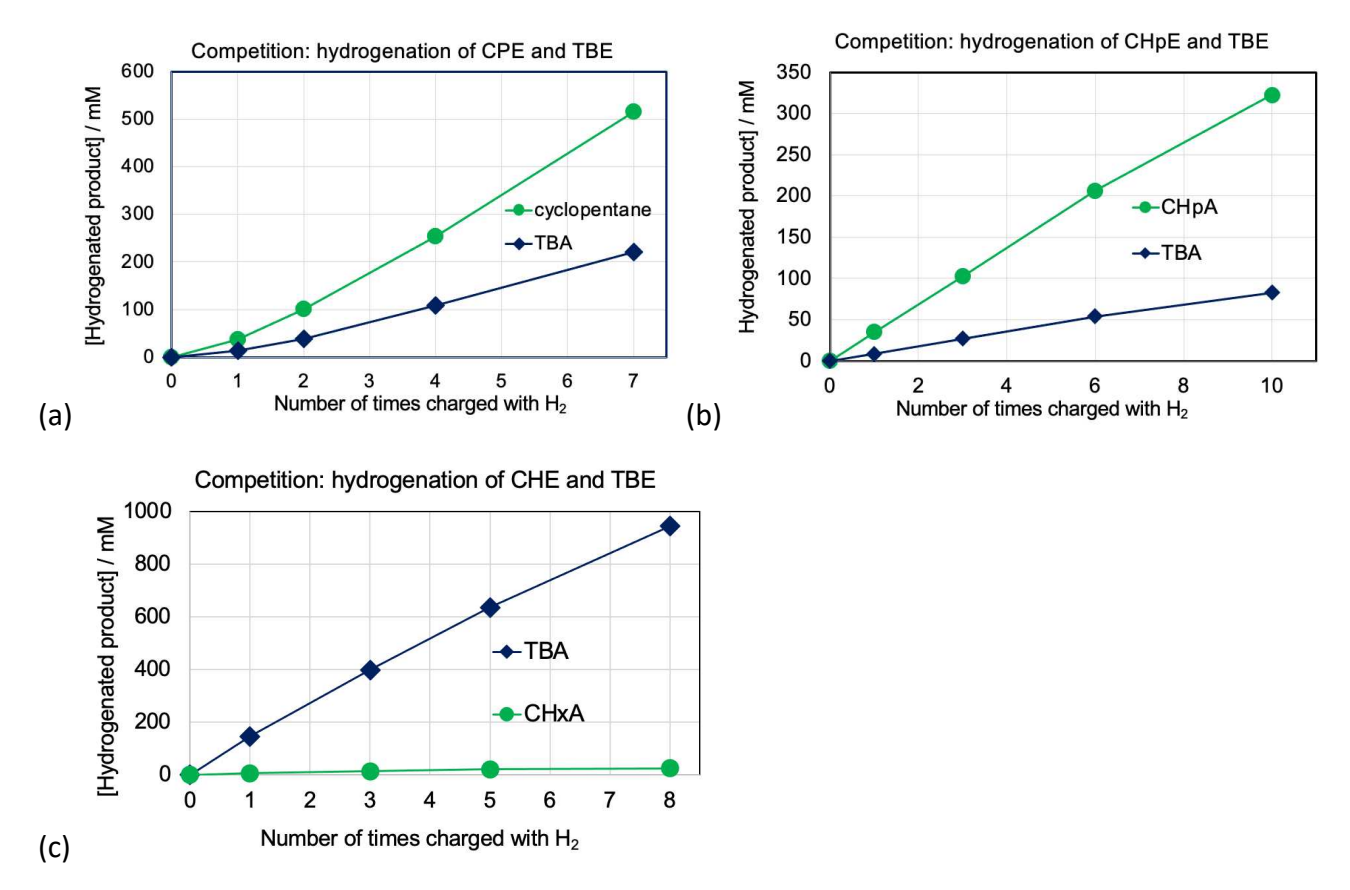


Figure 9. (a) Competition experiments, hydrogenation catalyzed by (^{iPr}PCP)IrH+ (a) CPE versus TBE, (b) CHpE versus TBE, (c) CHxE versus TBE

CHxE has a thermodynamic driving force for hydrogenation *greater* than that of COE, CHpE, and CPE, by 3.5, 2.0 and 1.2 kcal/mol, respectively (Table 2). As noted above, CHpE and CPE are hydrogenated by ($^{\text{iPr}}$ PCP)IrH $^+$ faster than TBE while hydrogenation of COE and TBE proceed at essentially the same rate. Yet despite the significantly *more favorable* thermodynamics of hydrogenation of CHxE, the rate of CHxE hydrogenation was ca. 300-fold *slower* than that of TBE, corresponding to $\Delta\Delta G^{\ddagger} \approx 3.4$ kcal/mol favoring the hydrogenation of TBE over CHxE (and therefore also $\Delta\Delta G^{\ddagger} \approx 3.4$ kcal/mol favoring hydrogenation of COE over CHxE; Figure 10). Expressed in terms of *dehydrogenation*, this implies that the barrier to COA dehydrogenation is ≈ 6.9 kcal/mol less than for CHxA dehydrogenation (Figure 10) although the thermodynamics of COA dehydrogenation are only 3.5 kcal/mol more favorable.

Table 2. Relative thermodynamics of hydrogenation, activation free energies of hydrogenation (kcal/mol) of cycloalkenes/cycloalkanes catalyzed by **1-H**⁺ (expressed relative to TBE/TBA), and inferred relative activation free energies and rates of dehydrogenation

Alkane	ΔΔG° hydrogenation	Relative rate hydrogenation of alkene	$\Delta\Delta G^{\ddagger}$ hydrogenation	$\Delta\Delta G^{\ddagger}$ dehydrogenation	Relative rate of dehydrogenation of alkane (inferred)
ТВА	(0.0)	(1.0)	(0.0)	(0.0)	(1.0)
cyclopentene	+3.3	2	-0.4	-3.7	520
cyclohexene	+2.1	0.003	+3.4	+1.3	0.11
cycloheptene	+4.1	4	-0.8	-4.9	3900
cyclooctene	+5.6	1.0	0.0	-5.6	13000

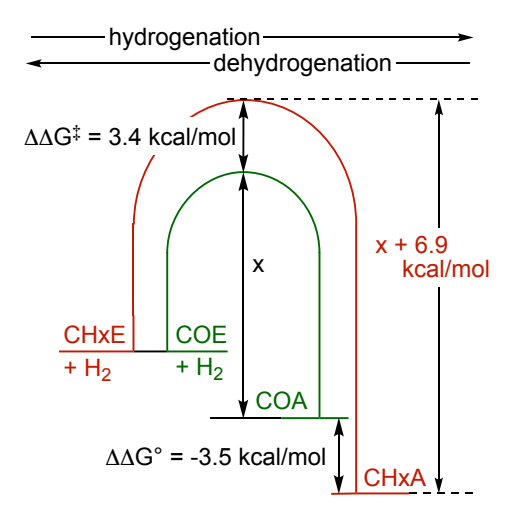


Figure 10. Schematic illustration of relative kinetic barriers of dehydrogenation of CHxA and COA catalyzed by **1-H**⁺ inferred from the kinetics of hydrogenation of CHxE and COE by **1-H**⁺ and the known relative thermodynamics.

Competition H/D Exchange Catalysis using 1-H $^+$. Alkane dehydrogenation by molecular transition metal catalysts is generally accepted to proceed via C-H oxidative addition followed by β -H-transfer. ^{11, 37-38} With the goal of probing the C-H activation step, we conducted H/D exchange experiments, again relying on competition experiments to avoid confounding effects due to varying the resting state (particularly as a result of varying the nature of olefinic products) or due to the possible presence of impurities in any particular reagent/substrate.

H/D exchange experiments were based on competitions between various deuterated alkanes versus benzene-d₆. With H₂ as the source of hydrogen and the reaction monitored by ¹H NMR

spectroscopy, $\mathbf{1}$ - \mathbf{H} ⁺ (generated from $\mathbf{1}$ - \mathbf{HCl} and Na[BArF²⁴]) was found to catalyze H/D exchange with benzene ca. 3-fold more rapidly on a per mol basis than with CHxA (Figure 11a). H/D exchange with n-octane proceeded about 2.4 times more rapidly on a per mol basis, with a slight regioselectivity for the terminal position (per C-D bond; Figure 11b).

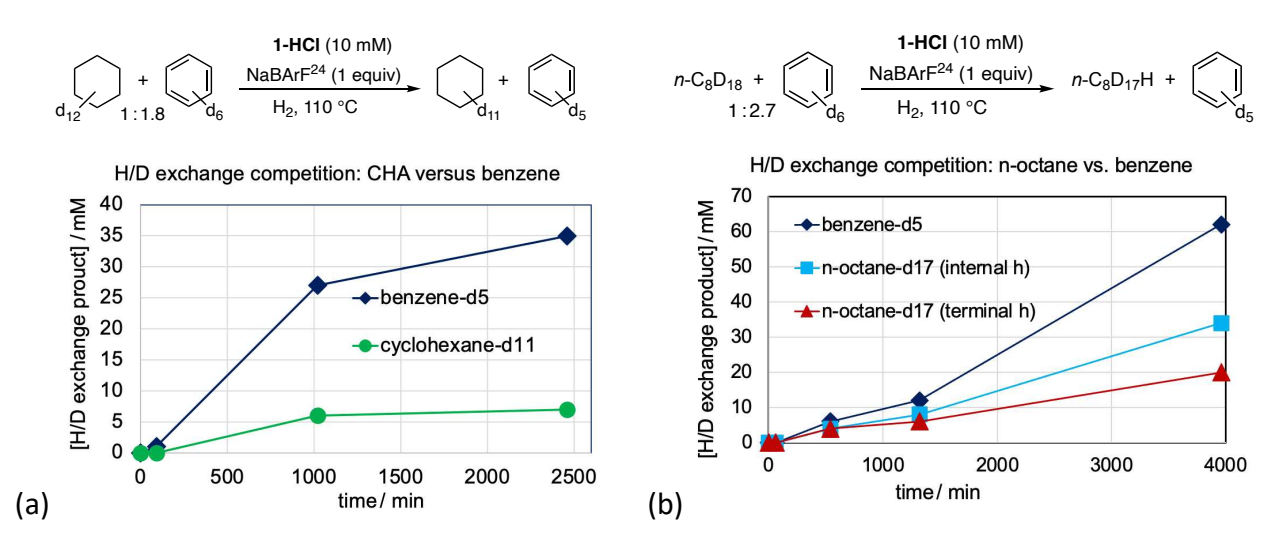


Figure 11. H/D exchange using H_2 as the source of hydrogen; competitions versus benzene- d_6 (a) cyclohexane- d_{12} (b) n-octane.

In a striking contrast to the selectivity for H/D exchange of benzene over CHxA, an analogous competition experiment with COA instead of CHxA revealed very high selectivity for COA, over 50:1 on a per mol basis (Figure 12a). Similar results were obtained when dioxane- h_8 was used instead of H_2 as the hydrogen source (Figure 12b).

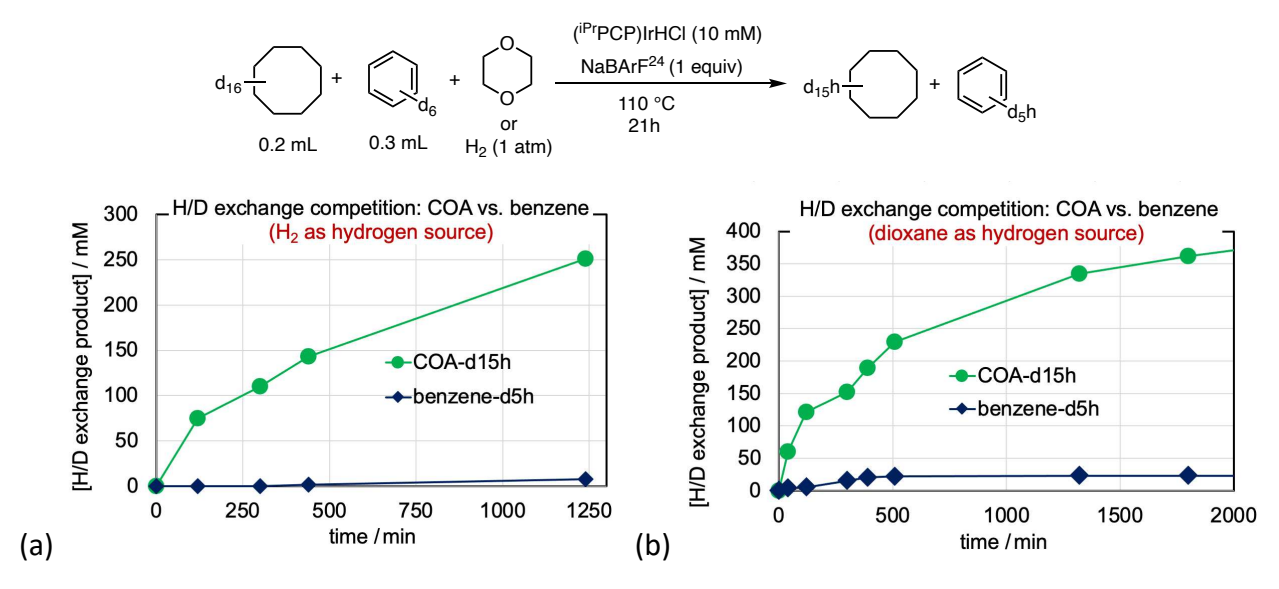


Figure 12. H/D exchange competition studies for cyclooctane- d_{16} using as the source of hydrogen (a) H_2 , and (b) dioxane- h_8 .

Intramolecular H/D exchange competition experiments were also conducted. When H/D exchange of toluene was effected with **1-H**⁺, it was found that the meta- and para-positions were equally reactive on a per-bond basis, while no exchange was observed at the orthoposition presumably due to steric crowding (Figure 13a). The meta- and para-positions are significantly (ca. 8-fold) more reactive than the benzylic position of toluene. In surprising contrast with toluene, however, the benzylic position of ethylbenzene is ca. 1.5-fold more reactive than its meta- and para-positions (Figure 13b); the benzylic position of ethylbenzene is thus about 12-fold more reactive than the toluene benzylic position. Moreover, also surprisingly, the methyl group of ethylbenzene is about 1.5-fold more reactive than the methylene group of ethylbenzene; the ethylbenzene methyl group is therefore more reactive by a factor of ca. 18 than the toluene (benzylic) methyl group. (These comparisons assume that the respective aromatic C-D bonds of toluene and ethylbenzene are approximately equally reactive).

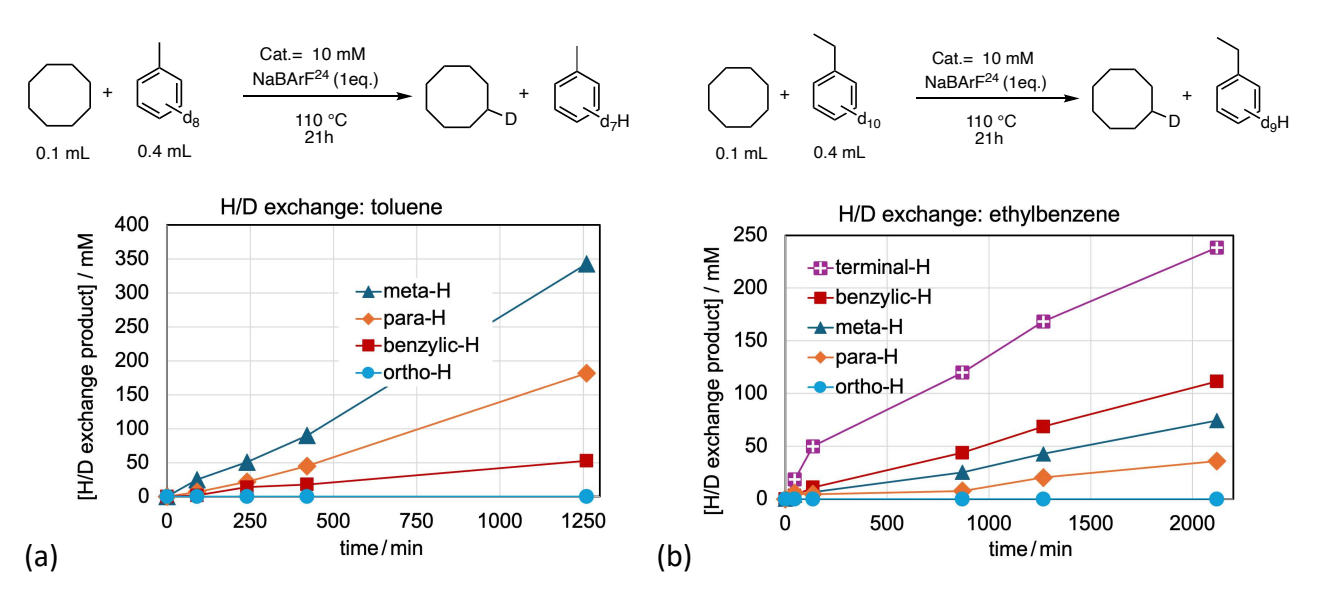


Figure 13. H/D exchange intramolecular competition studies for toluene- d_8 and ethylbenzene- d_{10} , using COA the source of hydrogen.

Olefin binding. Small crystals were obtained from the NMR tube in which hydrogenation of COE and TBE (Figure 8a) was catalyzed by [1-H⁺][BArF²⁴]. scXRD afforded the molecular structure of [(^{iPr}PCP)IrH(OH₂)(COE)][BArF²⁴] (Figure 14), suggestive of a resting state [(^{iPr}PCP)IrH(COE)⁺] (1-H(COE)⁺). The source of water observed in the crystal structure was not determined but we suspect it to be the Na[BArF²⁴] used to generate [1-H⁺][BArF²⁴] from 1-HCI.

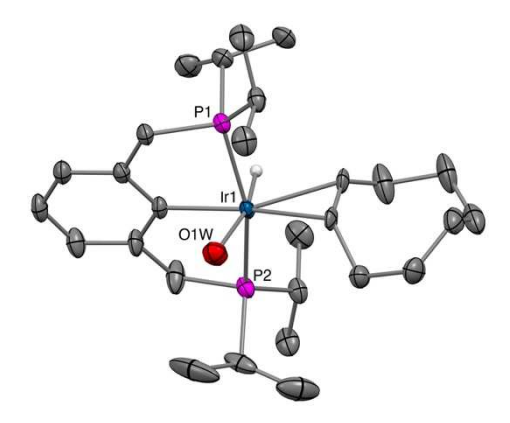


Figure 14. Molecular structure of cationic component of [1-H-COE(H₂O)][BArF²⁴] determined by scXRD. BArF²⁴ anion and hydrogen atoms, except for the hydride ligand, omitted for clarity.

■ DFT COMPUTATIONS AND MECHANISTIC DISCUSSION

The behavior of the present system contrasts dramatically with trends generally seen in studies of C-H activation by transition metal complexes. For example in Bergman's seminal reports on oxidative addition of alkane C-H bonds the relative order of reactivity was found to be benzene (4.7) > n-alkane 1° (2.7) > CPA (1.6) > CHxA (1.0) > COA (0.09). $^{4-5}$, $^{40-41}$ Since that time, many systems have been reported in accord with this general trend. $^{42-52}$ By contrast, we find that COA undergoes H/D exchange at least 30-fold faster than benzene in the present system, and over 150-fold faster than CHxA. The observation that dehydrogenations of COA and CPA are more facile than that of CHxA is perhaps not surprising as it is consistent with the relative thermodynamics of dehydrogenation — but the magnitude of the differences is much too high to be explained primarily in terms of thermodynamics. This point is reflected in the observation that COE, CHpE, and CPE also undergo *hydrogenation* much faster than CHxE, or even TBE, in spite of the fact that hydrogenations of the former olefins are thermodynamically *less* favorable. This very unusual selectivity, observed for both H/D exchange and for dehydrogenation/hydrogenation, has been investigated by computational (DFT) methods.

Geometry optimization and vibrational analyses were carried out in the gas phase using the M06L density functional as implemented in *Gaussian-16*.⁵³⁻⁵⁴ For this purpose the 6-311G(d,p) basis set was used for the main group elements,⁵⁵ while iridium carried the SDD relativistic effective core potential and associated basis set augmented with one f polarization function. 56-⁵⁷ Final electronic energies were obtained in a polarizable continuum representing toluene as solvent⁵⁸ via single point calculations on the gas-phase geometries using the M06L, ωB97X-D,⁵⁹ B3LYP-D3BJ⁶⁰ and PBEO-D3BJ ⁶¹⁻⁶² density functionals, employing this time the def2-tzvp basis set on the main group elements and the def2-qzvp basis set with associated ECP on Ir. 63-64 The enthalpy and Gibbs free energy terms were obtained from the gas phase calculations at 298.15 K and adjusted to 1M. 65-66 The computed gas-phase entropies for associative/dissociative reactions were exaggerated and exhibited large variations among related reactions; to mitigate these effects, the entropies were scaled by 0.5.67 Values differed among the different functionals, but similar trends were found for the entire range of alkanes investigated. We base the discussion on the M06L results. The ^{iPr}PCP ligand can define several conformation; for practical considerations we limited the calculations to the conformer observed for [1-H-COE(H₂O)][BArF²⁴] in Figure 14.

C-H Bond Addition. The d⁶-(PCP)IrH⁺ fragment is calculated to have a closed shell electronic state and a bent geometry. Calculated transition states (TSs) for C-H addition to **1-H**⁺ (**TS1**), for all alkanes investigated, are illustrated in Figure 15. The C-H bond undergoing cleavage can in principle be oriented with H pointing either toward or away from the hydride ligand of **1-H**⁺. We will first discuss pathways in which the H of the cleaved C-H bond is oriented away from the hydride (this will be designated as Mechanism **A** when distinguishing it from pathways that proceed via the alternative orientation, to be discussed below). In all cases the incipient Ir-H and Ir-C bonds are found to be nearly fully formed in the TS. The incipient Ir-H bond distances are essentially equal (within 0.02 Å) to the Ir-H bond distance of the hydride ligand already present prior to C-H addition (Figure 15). Likewise, the incipient Ir-C bond is quite short, ca. 2.2 Å, within the range of a typical iridium alkyl C-H bond length. Accordingly, the C-H distance of the bond undergoing cleavage in the TS (>1.75 Å) is far greater than that of an actual C-H bond. Thus the C-H addition TSs are quite "late", and have substantial Ir(V) character.

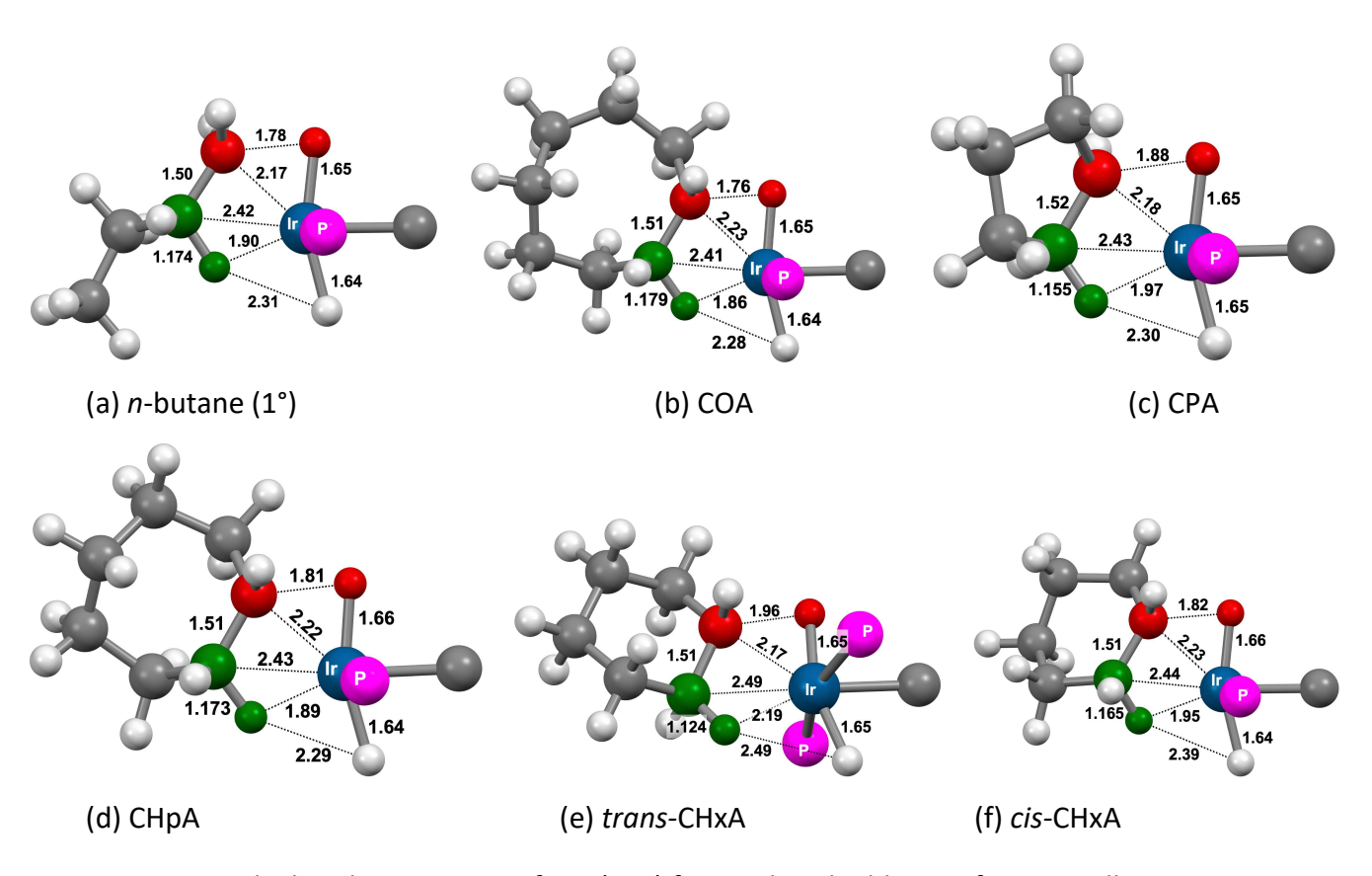


Figure 15. Calculated geometries of TSs (**TS1**) for C-H bond addition of various alkanes, as indicated. Atoms of C-H bond undergoing addition in red and the atoms of the β -agostic C-H bond in green.

The most noteworthy aspect of the TSs for C-H addition is an agostic interaction with the β -C-H bond (Figure 15). This interaction appears to be very strong as indicated by the pronounced elongation of the β -C-H bond as well as the short β -H-Ir bond distance. Respective values, for example in the case of *n*-butane (Figure 15a), are 1.174 Å (versus 1.09 Å for a typical alkyl C-H bond), and 1.90 Å (M-H bond distances of agostic C-H bonds are considered to range between 1.8 and 2.3 Å.⁶⁸) For addition of COA, the strength of the agostic interaction appears to be nearly equal (very slightly greater) to that for *n*-butane (respective C-H and β -H-Ir bond distances are 1.179 and 1.86 Å; Figure 15b). Likewise, similar values are found for cyclopentane (β -C-H and β -H-Ir distances of 1.155 and 1.97 Å, Figure 15c), while distances for cycloheptane (CHpA) are essentially identical to those calculated for *n*-butane (Figure 15d).

In the case of cyclohexane C-H addition we have located two isomeric TSs for C-H addition. In the lower energy isomer, the C-H bond undergoing addition and the agostic β -H are at trans positions of the six-membered ring (Figure 15e), in contrast to the TSs for the aforementioned cycloalkanes in which Ir and the agostic β -hydrogen are mutually cis (Figures 15b-d). The metrics of the Ir-C-H β -agostic unit of this species indicate an agostic interaction significantly weaker than for the other alkanes, although the metrics of the C-H bond undergoing cleavage are very similar to those of the other three substrates. In the second TS for cyclohexane C-H addition, the C-H bond undergoing cleavage and the agostic β -C-H bond are mutually cis (Figure 15f). The metrics of this *cis*-CHxA TS, both those of the agostic Ir-C-H unit and the C-H bond undergoing addition, are very similar to those found in the other alkanes; the *cis*-CHxA TS, however, is of slightly *higher* energy than the *trans*-CHxA TS, in spite of the much more pronounced agostic interaction found in the former.

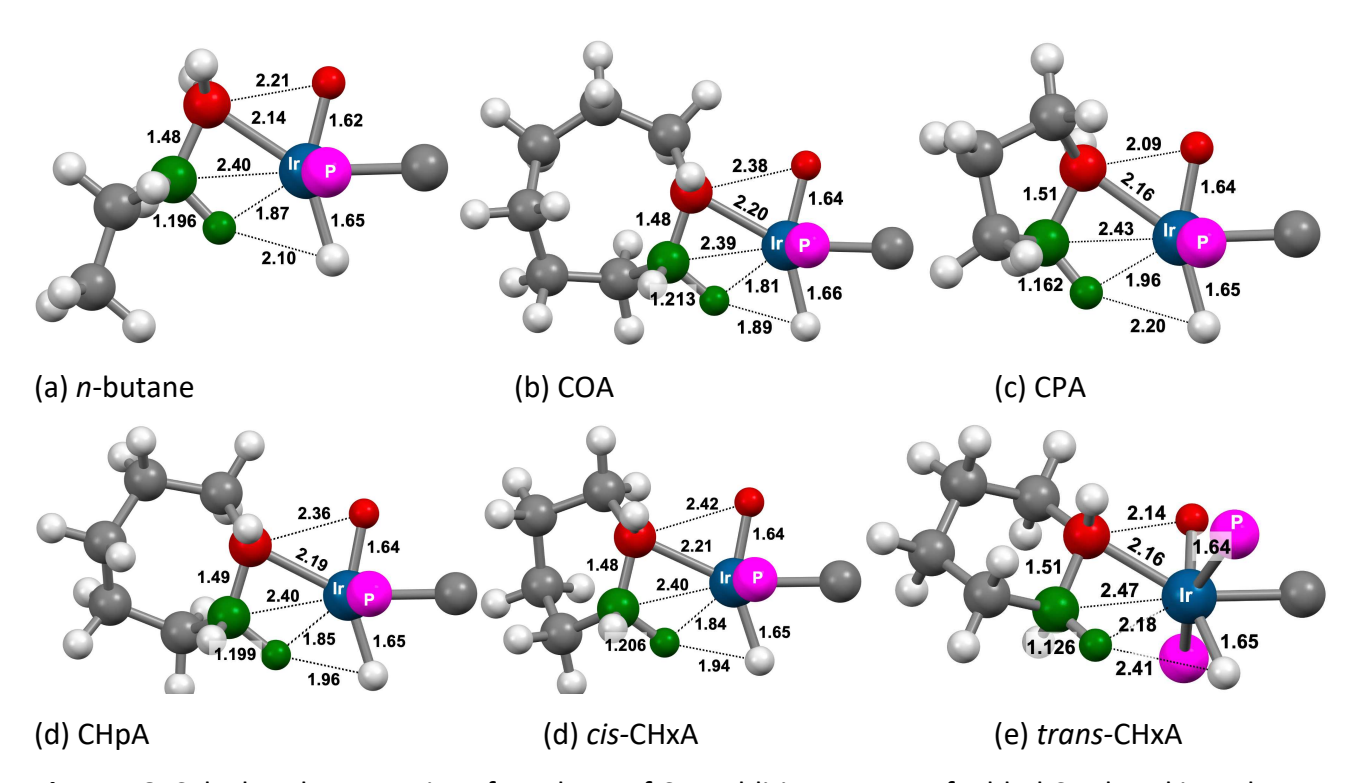


Figure 16. Calculated geometries of products of C-H addition. Atoms of added C-H bond in red and the atoms of the β -agostic C-H bond in green.

The calculated products of the C-H additions of *n*-butane, COA, CPA, CHpA, and CHxA (cis) (Figure 16 a-d) show agostic interactions that in general appear to be even stronger than those found in the respective TSs; the agostic Ir-H distances are shorter and the agostic C-H bonds are longer. In the case of the trans isomer of CHxA C-H addition (Figure 16f), however, these distances are unchanged (within 0.002 Å) from the TS; thus the weak agostic interaction in the trans-TS for cyclohexane addition remains weak in the corresponding trans C-H addition product. Despite this apparently much weaker agostic interaction, the trans C-H addition product is approximately the same energy as the cis isomer (Table 2). The explanation for this seems clear. In the trans isomers of both TS and intermediate (Figures 14e and 15e), the CHxA unit has the very stable chair conformation, while in the cis isomers the ring is severely twisted. Thus, CHxA can "choose" either a strong agostic interaction, similar to that found with the other alkanes investigated, but accompanied by severe conformational strain (the cis conformer), or alternatively, an unstrained trans conformer with a weak agostic interaction. The energetic cost is comparably high for either "choice", for both TS and C-H addition product.

We believe that these isomeric CHxA species provide valuable insight into the factors that determine the energies of the cycloalkane dehydrogenations in general. Note, however, that only the cis species are chemically relevant: the trans isomers can ultimately lead only to *trans*-cyclohexene – which is much too high in energy (free or bound) to be a viable product (Table 3).

Table 3. Calculated free energies of TSs and products of C-H addition to **1-H**⁺ (relative to free alkane and **1-H**⁺) and calculated enthalpy of free alkane in eclipsed conformation relative to unconstrained free alkane

	TS1 (C-H addition)	1-(H)₂R⁺ (C-H addition prod.)	TS2 (β-H- transfer)	1-H(H ₂)(alkene) ⁺ (β-H transfer prod.)	Ring strain	ΔH Eclipsed Conformer
TBA	15.0	15.0	18.9	6.7		2.1
<i>n</i> -butane	14.0	13.8	15.7	3.0		2.4
СРА	14.9	14.9	15.7	1.9	6.5	0.0
CHxA (cis)	22.5	20.5	20.7	3.9	0.0	9.8
CHxA (trans)	20.8	21.4	35.0	32.0	0.0	n/a
СНрА	14.3	12.5	13.8	1.7	6.3	0.6
COA	12.3	9.7	9.8	1.2	9.6	1.8

Whereas CHxA must undergo severe strain to adopt a conformation allowing a strong agostic interaction, essentially the opposite is true for the other cycloalkanes investigated. The agostic interaction requires an unfavorable eclipsed relationship of the H atoms that are geminal to the agostic C-H bond and the Ir center. This is necessarily unfavorable, but it results in overall relief of the ring strain found in free CPA, CHpA, and COA. In support of this proposal, calculations of the free cycloalkanes with a fully eclipsed HCCH unit (Table 3) indicate an energetic cost of 9.8 kcal/mol for CHxA, much greater than that of *n*-butane (2.4 kcal/mol). In contrast, the energies of eclipsed conformers of CPA, CHpA, and COA are *lower* than that of *n*-butane.

Calculated activation and reaction free energies and enthalpies of the C-H additions are shown in Table 3. Consistent with the TSs of C-H addition being "very late" (as reflected in the nearly full formation of Ir-C and Ir-H bonds as well as nearly full cleavage of the C-H bonds), the free energies of the products of addition are nearly equal to those of the TSs, or even very slightly higher⁶⁹. The span of ca. 10 kcal/mol in ΔG^{\ddagger} and 12 kcal/mol in ΔG° are both far greater than implied by previously reported experimental studies^{4-5, 40-43, 52} of cycloalkane addition (e.g.

a range of 12-fold between CPA, CHxA, and COA at -60 °C, corresponding to a difference of only ca. 1.1 kcal/mol). Perhaps even more notably, COA was found to be the *least* reactive cycloalkane in such systems, while COA is calculated to be the most reactive in the present one. These differences can be well explained, as discussed above, in terms of ring strain and the importance of the agostic interaction in the present system. Conversely, in the case of "classical" C-H activating transition metal systems, where no ancillary agostic interaction is involved, the addition of a metal center to the ring only *increases* the strain associated with eclipsed or intra-annular interactions.

 β -H Transfer. For catalytic alkane dehydrogenations operating via an initial C-H bond addition, the mechanism is typically assumed to proceed by a conventional of β -H transfer step, to afford a coordinated olefin and an M-H bond. Our calculations however predict that the agostic β -C-H bond in the α -C-H addition products, instead undergoes a transfer of the β -H to the adjacent hydride ligand; no intermediate with an Ir-H bond is formed during this process. Such β -H-transfers to a ligand are not common, but they are not unprecedented. The Ir-(β -H) distances (ca. 1.71 Å), however, indicates a significant degree of Ir-H bonding in these TSs (Figure 17). Perhaps the closest comparison to such a TS is with oxidative hydrogen migrations or α -CAM pathways the the TS typically has character of a C-H addition product but rather than being an energy minimum it is a TS leading to a dihydrogen complex.

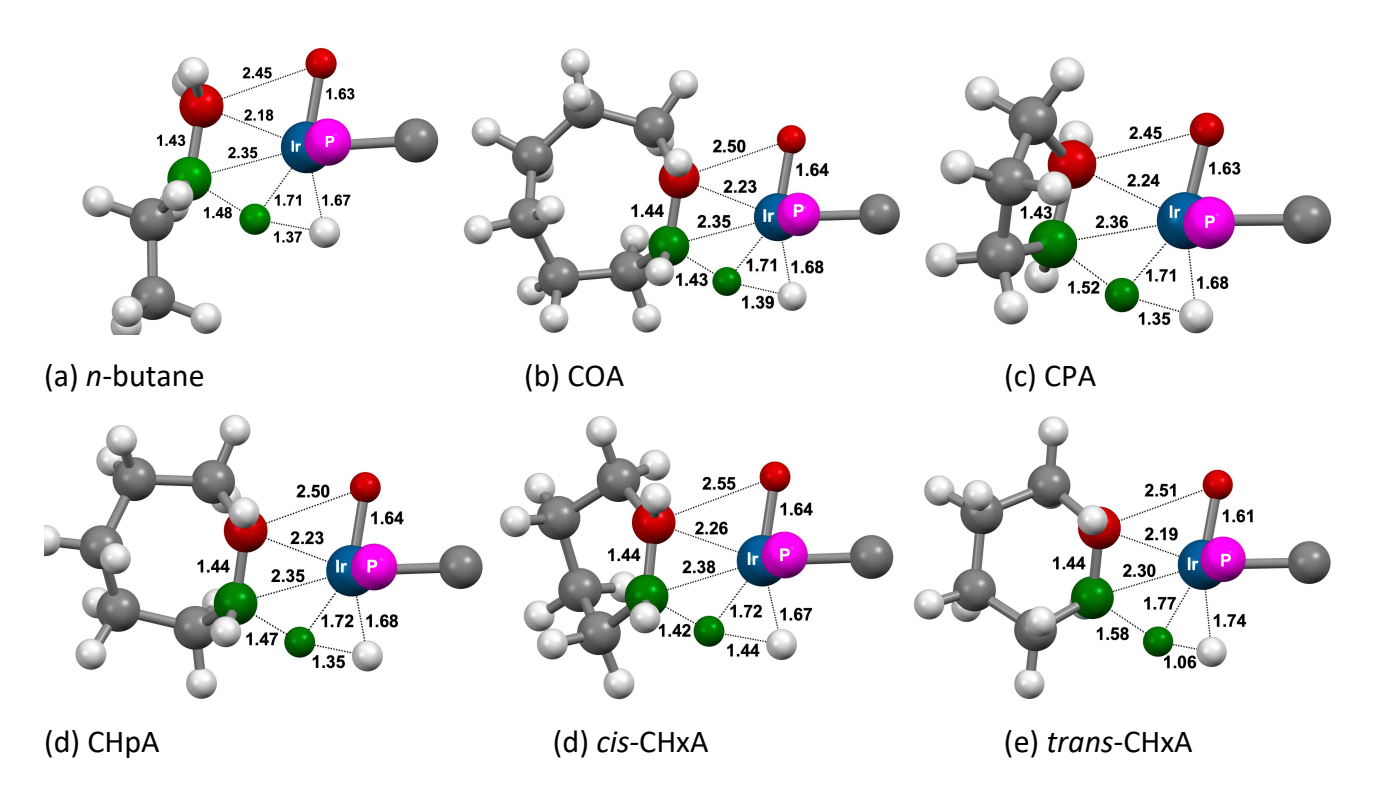


Figure 17. Calculated geometries of TSs for β -C-H transfer (from carbon to hydride). Atoms of C-H bond undergoing addition in red and the atoms of the β -agostic C-H bond in green.

As stressed above, the TSs for C-H addition (**TS1**) have geometries and energies remarkably similar to the C-H addition products (**i1**). Those same C-H addition products have geometries and energies very similar to the subsequent TSs (**TS2**) for β -H-transfer to hydride (geometric relationships are highlighted in Figure 18 for cyclopentane; see Table 3 for free energies). Given how shallow are these calculated minima on the energy surface, we can infer that they do not represent true intermediates, in the sense of species with a finite lifetime. Rather, the C-H addition and β -H transfer to hydride can be viewed, in effect, as components of an asynchronous concerted process, ⁷⁸⁻⁷⁹ connecting weakly bound alkane σ -C-H complex precursors (**1-H(RH)**⁺) with the corresponding olefin dihydride complex intermediates **1-H(alkene)(H₂)**⁺.

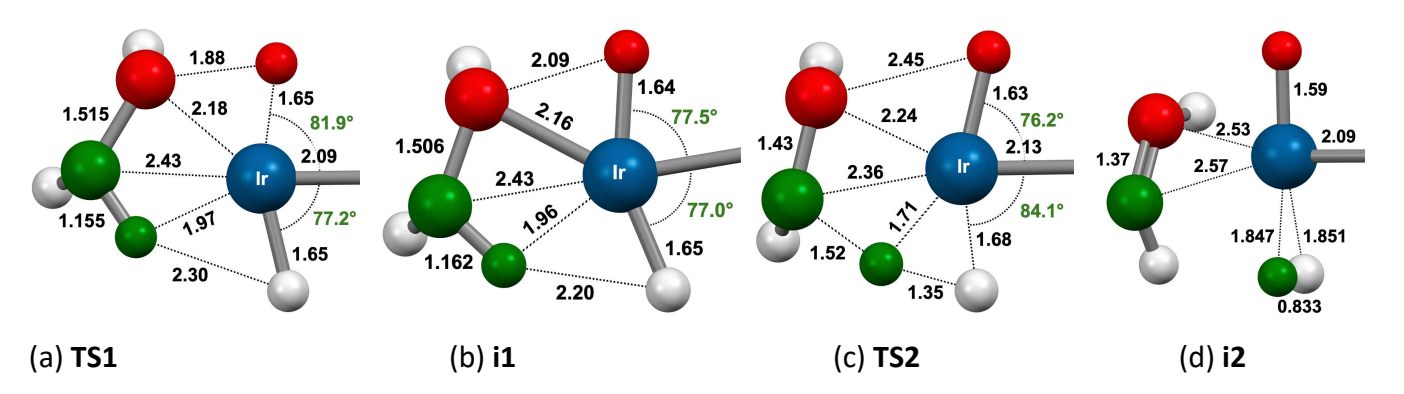


Figure 18. Dehydrogenation of cyclopentane by **1-H**⁺ illustrating the geometric similarity of (a) the TS for C-H addition (**TS1**) (b) the energy minimum (**i1**) reached via IRC from **TS1** (c) the TS for β-H transfer from carbon to hydride (**TS2**); and the intermediate (**i2**) reached via IRC from **TS2**. For clarity, only atoms in the coordination sphere of the metal and approximately in the plane perpendicular to the P-P axis (and H atoms bound to the key carbons undergoing C-H addition and β-H transfer) are shown.

The products derived from **TS2**, **1-H(alkene)(H₂)**⁺ (e.g. Figure 18d), have very short (ca. 0.83 Å) H-H distances, with the H₂ ligand oriented perpendicular to the plane of the reaction coordinate of the β -H transfer TS.

Following the formation of **1-H(alkene)(H₂)**⁺, several different steps appear to be plausible. The formation of **1-H(alkene)(H₂)**⁺ from alkane and **1-H**⁺ is calculated to be endergonic in all cases (Table 3; Figure 20); therefore, the reverse of its formation would be rapid. Rotation of H₂ around the (η^2 -H₂)-Ir axis presumably has a very low barrier. The formation of **1-H(alkene)(H₂)**⁺, followed by a rapid back-reaction, would therefore lead to exchange between the hydride of **1-H**⁺ and alkane, providing a pathway for hydrogen isotope exchange (HIE). Notably the *H/D* exchange occurs at the β -position rather than at the site of actual (α) *C-H* addition (Figure 19).

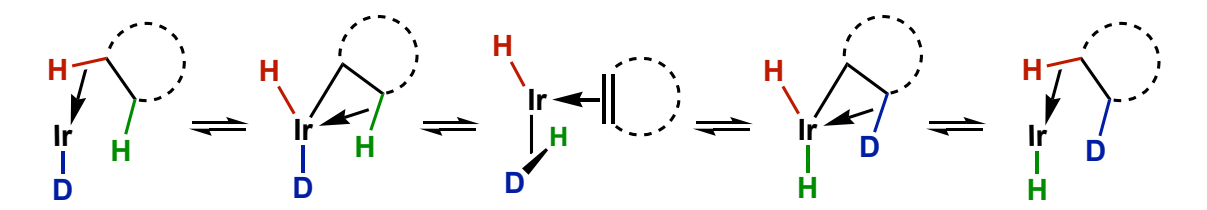


Figure 19. Schematic illustration of Mechanism A for H/D exchange

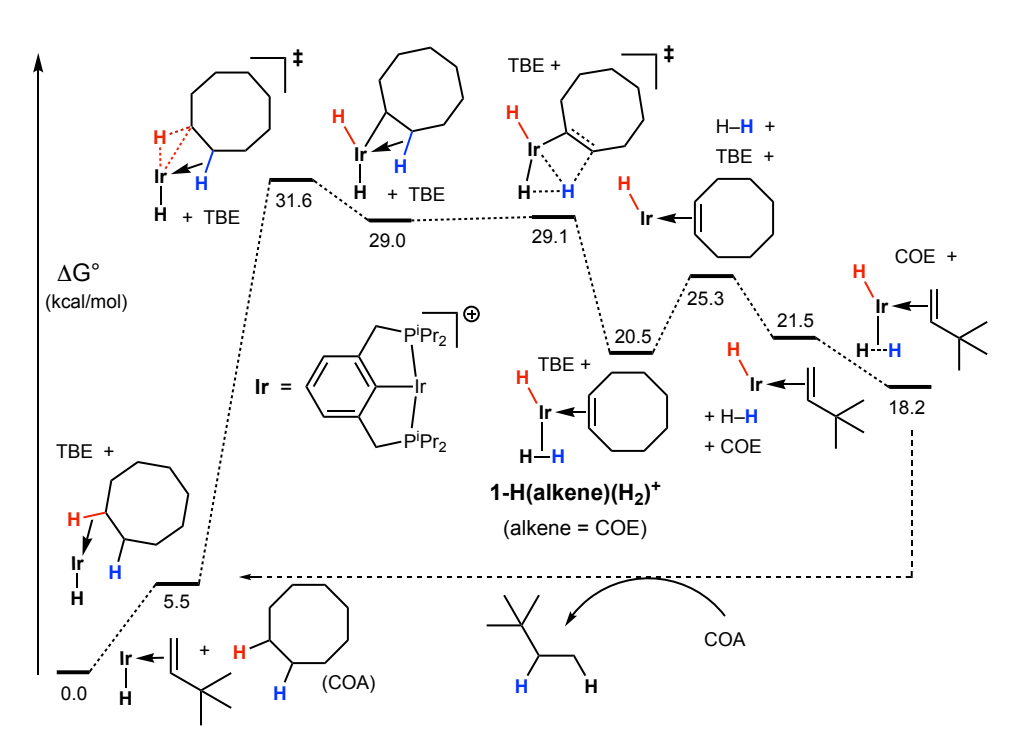


Figure 20. Free energy profile and schematic of full catalytic cycle for COA/TBE transferdehydrogenation

Loss of H_2 from **1-H(alkene)(H_2)**⁺ is calculated to be only moderately endothermic (ΔH° = ca. 10 kcal/mol) and slightly endergonic (Figure 20). We have been able to locate a TS for loss of H_2 from only one of the **1-H(alkene)(H_2)**⁺ complexes (alkene = 1-butene) but, as expected, the kinetic barrier for H_2 loss is only slightly higher than the low thermodynamic barrier and thus H_2 loss is presumably facile and reversible. We infer that this is the case for all the alkanes studied.

If H₂ is lost reversibly from **1-H(alkene)(H₂)**⁺, the H₂ loss process would have no obvious effect on any of the experimental observations including HIE. However, H₂ loss results in a vacant coordination site which could permit an associate exchange of alkenes. Indeed, as discussed in the previous section (Experimental Results), experimentally we have shown that complexes **1-H(alkene)(H₂)**⁺ undergo rapid exchange between free and bound alkene. If alkene exchange does occur prior to re-association of H₂, followed by hydrogenation of the incoming alkene to give the corresponding alkane (the reverse of the alkane dehydrogenation), it provides a full pathway for transfer dehydrogenation (with COA/TBE as the H-donor/H-acceptor couple in Figure 20). We also cannot rule out an alternative catalytic pathway for alkene

exchange, in which alkene is lost directly from **1-H(alkene)(H₂)**⁺ and the incoming acceptor replaces it (COE and TBE in Figure 20). Loss of alkene, however, is calculated to be substantially more endergonic than loss of H₂, e.g. ΔG° = 16.6 kcal/mol for COE, compared with ΔG° = 4.8 kcal/mol for loss of H₂. But regardless of whether alkene exchange occurs directly, or via loss of H₂ (as in Figure 20), if exchange is rapid relative to the back reaction for formation of **1-H(alkene)(H₂)**⁺ it would not affect the overall rate of transfer-dehydrogenation (or HIE). This study is focused primarily on the initial C-H bond cleavage and β -H transfer steps, i.e. the formation of **1-H(alkene)(H₂)**⁺ from **1-H**⁺ and alkane. In view of the unusual selectivity it is clear that these steps, and not olefin exchange, determine the rates, including relative rates, of dehydrogenation and HIE.

Note that in all cases discussed above, the C-H bond undergoing addition is positioned trans to the hydride ligand initially present in **1-H(RH)**⁺, while the agostic bond is cis to that hydride (Figure 15). This represents an unusual pathway in which the exchange occurs *between the originally present hydride ligand and the \beta-C-H bond for all alkanes discussed above. Such a pathway, however, is not possible or favorable for species that cannot feasibly undergo 1,2-dehydrogenation, e.g. for aromatic C-H bonds or for the benzylic C-H bond of toluene. Yet, as described in the experimental results section above, these molecules are in fact observed to undergo HIE, although somewhat slowly. In this context we now consider pathways in which the hydride resulting from C-H addition is positioned cis to the hydride initially present in 1-H⁺, thus allowing exchange between hydride and the \alpha-C-H bond*

Consideration of an alternative orientation of addition: Mechanism B. C-H addition with an orientation opposite that of the examples discussed above has been calculated for several of the same exemplary alkanes. It is found that C-H addition via this pathway (Mechanism B) initially proceeds similarly to that as discussed above (Mechanism A) (Figure 21). In particular, as in Mechanism A, there appears to be a strong β -agostic interaction in the C-H addition TS for Mechanism B. In this case, the β -agostic interaction is necessarily positioned cis to the PCP ipsocarbon and trans to the hydride present prior to C-H addition (Figure 21). Based on metric parameters, the agostic interactions, although relatively strong, appear to be slightly weaker than those present in the TSs of Mechanism A (i.e. the C-H distances are slightly shorter and the

Ir-C and Ir-H distances slightly longer; Figure 22). In the case of toluene, C-H addition proceeds via a TS with η^3 -allyl character, in which the C1-C2 π -system seems to play a role analogous to that of the agostic C-H bond for alkane C-H addition (Figure 22).

Figure 21. Schematic illustration of Mechanism **A** (C-H bond addition trans to the hydride ligand of $\mathbf{1}$ - \mathbf{H} ⁺) and Mechanism **B** (C-H bond addition cis to the hydride ligand of $\mathbf{1}$ - \mathbf{H} ⁺)

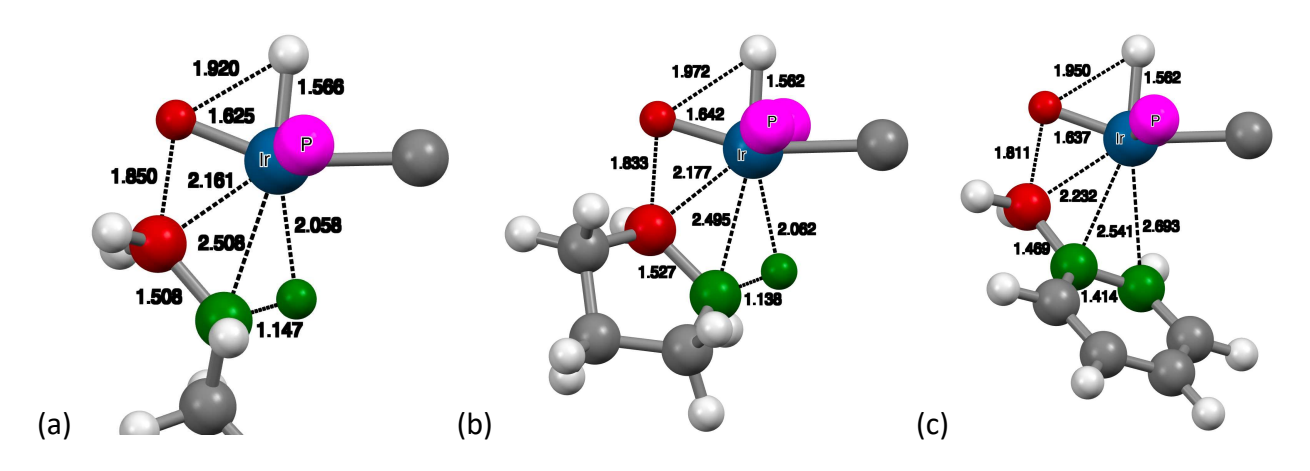


Figure 22. Calculated geometries of TSs for C-H addition of (a) n-butane (1°), (b) CPA, and (c) toluene (benzylic position) proceeding via Mechanism **B** (**TS1**^B). Atoms of C-H bond undergoing addition in red and the atoms of the β-agostic C-H bond (or C1-C2 π -system for toluene) in green. (See Figure 15 for Mechanism **A** analogues for n-butane (1°), and CPA.)

As in the case of Mechanism **A**, the products of C-H addition of Mechanism **B** are geometrically and energetically very similar to the TSs which lead to them (Figure 23). Other than the relative position of the hydride ligand that is present prior to addition, both the energies and the metric parameters of the TSs and products of C-H addition of Pathways **A** and

B are quite similar (Table 4). However, unlike Pathway **A**, Pathway **B** results in the two hydride ligands positioned mutually cis. This would seem to offer the possibility of facile reductive formation of coordinated H₂, which, if reversible, could result in HIE between **1-H**⁺ and alkane.

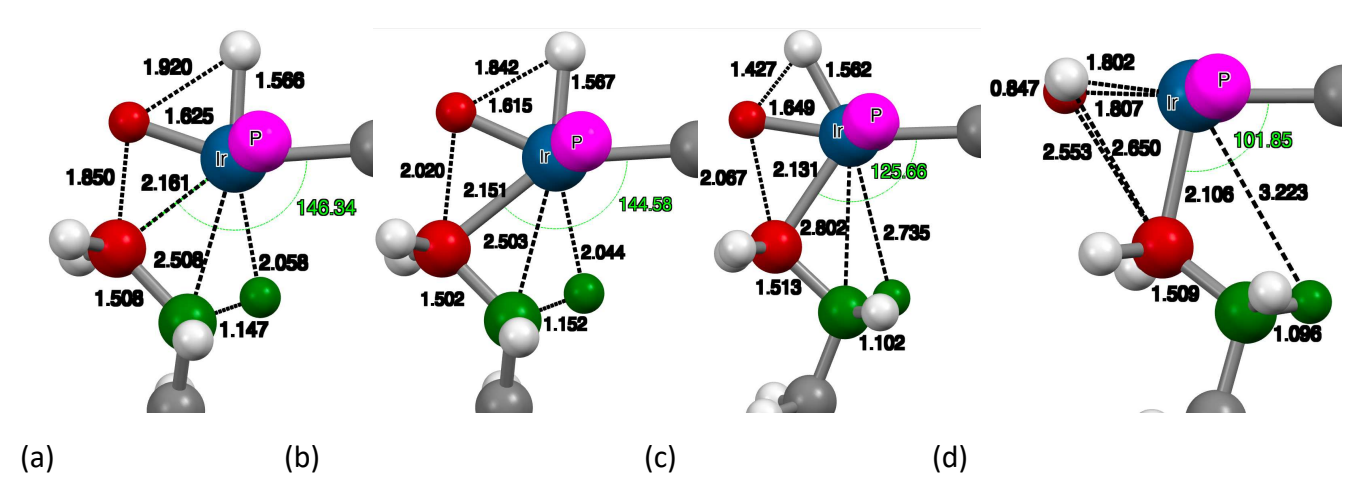


Figure 23. Reaction of $\mathbf{1}$ - \mathbf{H} ⁺ with n-butane (1° position) via Mechanism \mathbf{B} : (a) TS for C-H addition, (b) product of C-H addition, (c) TS for H-H reductive bond formation, (d) product of H-H reductive bond formation.

Table 4. Calculated free energies of TSs and products of C-H addition to $\mathbf{1}$ - \mathbf{H} ⁺ (relative to free alkane and $\mathbf{1}$ - \mathbf{H} ⁺) for Pathways \mathbf{A} and \mathbf{B} . For mechanism \mathbf{A} , the \mathbf{H}_2 adduct formed is $\mathbf{1}$ - \mathbf{H} (alkene)(\mathbf{H}_2)⁺. For mechanism \mathbf{B} , the \mathbf{H}_2 adduct formed is $\mathbf{1}$ -(\mathbf{H}_2)(alkyl)⁺.

	TS1 (C-H	1 (C-H 1-R(H) ₂ + (C-H TS		Products of H-H bond
	addition)	addition product)	formation)	formation (H ₂ adducts)
<i>n</i> -butane				
ΔG (A)	14.0	13.8	15.7	3.0
ΔG (B)	15.5	15.5	23.8	11.1
СРА				
ΔG (A)	14.9	14.9	15.7	1.9
ΔG (B)	16.9	17.2	19.6	9.9
CHxA (cis)				
ΔG (A)	22.5	20.5	20.7	3.9
ΔG (B)	21.3	21.6	21.3	16.1
COA				
ΔG (A)	12.3	9.7	9.8	1.2
ΔG (B)	10.2	10.8	19.2	9.3
benzene				
ΔG (A)	28.5 ^a	a		
ΔG (B)	16.9	16.7	19.8	
Toluene				
ΔG (A)	26.6	26.0		
ΔG (B)	13.1	13.4	20.4	

⁽a) The TS for cleavage of the benzene C-H bond via "Mechanism A" i.e. C-H bond cleavage with H oriented away from the hydride ligand, does not lead to oxidative addition or H-H bond formation, but leads instead to migration of H from benzene, to form a C-H bond with the ^{iPr}PCP ipso carbon.

C-H addition via Pathway **B** affords Ir(V) product cis-1-R(H)₂⁺. Reductive H-H bond formation to give Ir(III) dihydrogen complexes 1-R(H₂)⁺ is calculated to be thermodynamically downhill, e.g. for R = 1-butyl, ΔG° = -4.4 kcal/mol. Interconversion between cis-dihydride and dihydrogen complexes is typically kinetically very facile. However, there is a significant kinetic barrier to H-H bond formation (ΔG^{\ddagger} = 8.3 kcal/mol) in this case, and as a result, the TS for H-H bond formation (TS2^B) is significantly higher (also by 8.3 kcal/mol) in free energy than the TS for C-H addition (R = n-butyl, Table 4). This seems clearly attributable to the loss of the agostic interaction in the TS for H-H bond formation; this is required to achieve the favorable configuration of the product

 $1-R(H)_2^+$ (Figure 23 d) in which the two strong-trans-influence groups, the alkyl (R) and the PCP ipso-carbon, are mutually cis (>C-Ir-C = 102°).

Thus, alkane C-H addition is found to be comparably facile via Pathways **A** and **B**, with both pathways involving strong assistance by a β -agostic interaction. The resulting coordination geometries, however, then offer distinctly different possibilities for subsequent reactivity. Pathway **B** allows the reductive formation of bound H₂, and thereby enables direct HIE between the C-H bond that undergoes addition (α -C-H) and the hydride ligand of **1-H**⁺. Pathway **A** allows the transfer of H from the β -agostic C-H bond to the **1-H**⁺ hydride ligand (LLHT). Surprisingly perhaps, the LLHT TS (**TS2**^A) is very similar in energy and even geometry to the TS for C-H addition while the TS for H-H reductive bond formation (**TS2**^B) is significantly higher in energy. Thus the two pathways involve very different mechanisms for HIE, even resulting in HIE of different C-H bonds (i.e. the α - and β -C-H bonds for mechanisms **B** and **A** respectively).

Only in the case of Pathway **A** do the steps described above lead to dehydrogenation to give olefin (coordinated to the iridium center). In the case of Pathway **B**, β -H-transfer after C-H addition is in principle possible but if it were to occur after the H-H reductive bond formation (and subsequent H₂ loss) the overall barrier for the reaction would of course be at least as high as the TS for the H-H reductive bond formation step; the computational results strongly suggest that Pathway **B** is unfavorable for the alkanes investigated.⁸⁰

For C-H activation of substrates such as toluene (benzylic position) or benzene, Pathway **A** is not a feasible option for HIE. Either there is no β -H atom to transfer (following toluene benzylic activation) or β -H transfer would afford a very high-energy benzyne complex. We conclude that for these substrates, HIE (H/D exchange) proceeds via Mechanism **B**. The barriers calculated by DFT are quite consistent, within the expected accuracy limits, with these results. Thus the barrier to HIE exchange between benzene and **1-H** $^+$ via Mechanism **B** is greater than that calculated for COA via Mechanism **A** but less than that calculated for cyclohexane via either Mechanism **A** or **B** in accord with experimental findings (Figures 11 and 12). Likewise, the barrier to benzene HIE via Mechanism **B** is calculated to be less than that for the benzylic C-H bond of toluene, consistent with the more rapid exchange of para- and meta-C-H bonds of toluene versus exchange at the benzylic position. Notably, however, in the case of

ethylbenzene, exchange is more rapid at both benzylic and methyl group positions than at the para- and meta-positions; this can obviously be attributed to the viability of Mechanism $\bf A$ for ethylbenzene $C(sp^3)$ -H bonds in contrast with those of toluene.

■ SUMMARY AND CONCLUSIONS

The oxidative addition of C-H bonds by transition metal complexes and the dehydrogenation of alkanes proceeding via C-H oxidative addition have been studied extensively for over 40 years. In this work, we report an unanticipated role of a β -agostic bond in promoting C-H oxidative addition. The β -agostic C-H bond can then itself undergo activation, through a hydrogen transfer to a hydride ligand (LLHT), resulting in a 1,2-dehydrogenation of alkane to give a coordinated olefin and a dihydrogen ligand. This can result in HIE with the initially present hydride ligand if back-reaction follows, or the loss of free alkene and catalytic dehydrogenation in the presence of a sacrificial hydrogen acceptor. The energy surface of the overall process is calculated to have at most a very shallow energy minimum and the overall C-H addition and β-H-transfer leading to coordinated alkene may be considered an effectively asynchronous concerted process. 78-79 This pathway, which has no reported precedent to our knowledge, results in selectivity for both hydrogen isotope exchange (HIE) and catalytic dehydrogenation that is distinct from that of established systems for either of these reactions. Specifically, H-C-C-H linkages that favor the formation of β -agostic interactions undergo particularly facile HIE and catalytic dehydrogenation. Thus strained cycloalkanes (cyclopentane, cycloheptane, cyclooctane) undergo HIE more readily than benzene or the benzylic group of toluene, as well as HIE and catalytic dehydrogenation far more rapidly than cyclohexane or nalkane. Microscopic reversibility dictates that the same factors would favor hydrogenation and indeed the rates of cycloalkene hydrogenation are found to correlate positively with strain in the alkane product, and therefore correlate inversely with the thermodynamic driving force. In view of the importance of hydrogenation and dehydrogenation, as well as the great interest in C-H activation and HIE, we believe that these findings open potentially valuable new approaches to the design of catalysts based on consideration of β -agostic and perhaps other secondary interactions.

■ ASSOCIATED CONTENT

Supporting Information

Complete experimental details and synthetic procedures, NMR data, computational details and data, computed energies and thermodynamic quantities (PDF)

Optimized structures for calculated species (.mol format) (ZIP)

■ AUTHOR INFORMATION

Corresponding Authors

Alan S. Goldman – Department of Chemistry and Chemical Biology, Rutgers, The State
University of New Jersey, New Brunswick, New Jersey 08854, United States; orcid.org/00000002-2774-710X; Email: alan.goldman@rutgers.edu

Faraj Hasanayn – Department of Chemistry, American University of Beirut, Beirut 1107 2020, Lebanon; orcid.org/0000-0003-3308-7854

Authors

Ashish Parihar – Department of Chemistry and Chemical Biology, Rutgers, The State University of New Jersey, New Brunswick, New Jersey 08854, United States; orcid.org/0000-0003-1049-0077

Thomas J. Emge – Department of Chemistry and Chemical Biology, Rutgers, The State University of New Jersey, New Brunswick, New Jersey 08854, United States; orcid.org/0000-0003-4685-8419

Notes

The authors declare no competing financial interests

■ ACKNOWLEDGMENTS

We thank the U. S. Department of Energy Office of Science (DE-SC0020139) for support of this research. The National Science Foundation is acknowledged for grant CHE-2117792 for acquisition of the X-ray diffractometer used to obtain all scXRD structures for this work. Dr. Tarig Bhatti is thanked for highly valuable discussions at the outset of this work.

REFERENCES

(1) Crabtree, R. H.; Mihelcic, J. M.; Quirk, J. M., Iridium Complexes in Alkane Dehydrogenation *J. Am. Chem. Soc.* **1979**, *101*, 7738-7740. https://doi.org/10.1021/ja00520a030

- (2) Crabtree, R. H.; Mellea, M. F.; Mihelcic, J. M.; Quirk, J. M., Alkane dehydrogenation by iridium complexes *J. Am. Chem. Soc.* **1982**, *104*, 107-113. https://doi.org/10.1021/ja00365a021
- (3) Burk, M. J.; Crabtree, R. H.; McGrath, D. V., Thermal and Photochemical Catalytic Dehydrogenation of Alkanes with $[IrH_2(CF_3CO_2)(PR_3)_2]$ (R = C_6H_4F -p and cyclohexyl) *J. Chem. Soc., Chem. Commun.* **1985**, 1829-1830. https://doi.org/10.1039/C39850001829
- (4) Janowicz, A. H.; Bergman, R. G., Carbon-hydrogen activation in completely saturated hydrocarbons: direct observation of M + R-H -> M(R)(H) *J. Am. Chem. Soc.* **1982,** *104,* 352-354. https://doi.org/10.1021/ja00365a091
- (5) Janowicz, A. H.; Bergman, R. G., Activation of Carbon-Hydrogen Bonds in Saturated Hydrocarbons on Photolysis of (h⁵-C₅Me₅)(PMe₃)IrH₂. Relative Rates of Reaction of the Intermediate with Different Types of Carbon-Hydrogen Bonds and Functionalization of the Metal-Bound Alkyl Groups *J. Am. Chem. Soc.* **1983**, *105*, 3929-3939. https://doi.org/10.1021/ja00350a031
- (6) Burger, P.; Bergman, R. G., Facile intermolecular activation of carbon-hydrogen bonds in methane and other hydrocarbons and silicon-hydrogen bonds in silanes with the iridium(III) complex Cp*(PMe₃)Ir(CH₃)(OTf) *J. Am. Chem. Soc.* **1993**, *115*, 10462-10463. https://doi.org/10.1021/ja00075a113
- (7) Tellers, D. M.; Bergman, R. G., An Examination of C-H Bond Activation by Cationic TpMe₂Ir(III) Complexes *Organometallics* **2001**, *20*, 4819-4832. https://doi.org/10.1021/om010697c
- (8) Periana, R. A.; Liu, X. Y.; Bhalla, G., Novel bis-acac-O,O-Ir(iii) catalyst for anti-Markovnikov, hydroarylation of olefins operates by arene CH activation *Chem. Commun.* **2002**, 3000-3001. https://doi.org/10.1039/B208680H
- (9) Bhalla, G.; Liu, X. Y.; Oxgaard, J.; Goddard, W. A., III; Periana, R. A., Synthesis, Structure, and Reactivity of O-Donor Ir(III) Complexes: C-H Activation Studies with Benzene *J. Am. Chem. Soc.* **2005**, *127*, 11372-11389.
- (10) Choi, J.; Goldman, A. S., Ir-Catalyzed Functionalization of C–H Bonds *Top. Organomet. Chem.* **2011,** *34*, 139–167. http://dx.doi.org/10.1007/978-3-642-15334-1 6
- (11) Kumar, A.; Bhatti, T. M.; Goldman, A. S., Dehydrogenation of Alkanes and Aliphatic Groups by Pincer-Ligated Metal Complexes *Chem. Rev.* **2017**, *117*, 12357-12384. http://dx.doi.org/10.1021/acs.chemrev.7b00247
- (12) Ito, J.-i.; Kaneda, T.; Nishiyama, H., Intermolecular C-H Bond Activation of Alkanes and Arenes by NCN Pincer Iridium(III) Acetate Complexes Containing Bis(oxazolinyl)phenyl Ligands *Organometallics* **2012**, *31*, 4442-4449. http://dx.doi.org/10.1021/om3002137
- (13) Allen, K. E.; Heinekey, D. M.; Goldman, A. S.; Goldberg, K. I., Alkane Dehydrogenation by C-H Activation at Iridium(III) *Organometallics* **2013**, *32*, 1579-1582. http://dx.doi.org/10.1021/om301267c
- (14) Allen, K. E.; Heinekey, D. M.; Goldman, A. S.; Goldberg, K. I., Regeneration of an Iridium(III) Complex Active for Alkane Dehydrogenation Using Molecular Oxygen *Organometallics* **2014**, *33*, 1337-1340. http://dx.doi.org/10.1021/om401241e
- (15) Gao, Y.; Guan, C.; Zhou, M.; Kumar, A.; Emge, T. J.; Wright, A. M.; Goldberg, K. I.; Krogh-Jespersen, K.; Goldman, A. S., β-Hydride Elimination and C–H Activation by an Iridium Acetate Complex, Catalyzed by Lewis Acids. Alkane Dehydrogenation Cocatalyzed by Lewis Acids and [2,6-Bis(4,4-dimethyloxazolinyl)-3,5-dimethylphenyl]iridium *J. Am. Chem. Soc.* **2017**, *139*, 6338–6350. http://dx.doi.org/10.1021/jacs.6b12995
- (16) Zhou, X.; Malakar, S.; Dugan, T.; Wang, K.; Sattler, A.; Marler, D. O.; Emge, T. J.; Krogh-Jespersen, K.; Goldman, A. S., Alkane Dehydrogenation Catalyzed by a Fluorinated Phebox Iridium Complex *ACS Catal.* **2021**, *11*, 14194-14209. https://doi.org/10.1021/acscatal.1c03562
- (17) Bhatti, T. M.; Kumar, A.; Parihar, A.; Moncy, H. K.; Emge, T. J.; Waldie, K. M.; Hasanayn, F.; Goldman, A. S., Metal–Ligand Proton Tautomerism, Electron Transfer, and C(sp3)–H Activation by a 4-Pyridinyl-Pincer Iridium Hydride Complex *J. Am. Chem. Soc.* **2023**, *145*, 18296–18306. https://doi.org/10.1021/jacs.3c03376

(18) Wang, Y.; Huang, Z.; Liu, G.; Huang, Z., A New Paradigm in Pincer Iridium Chemistry: PCN Complexes for (De)Hydrogenation Catalysis and Beyond *Acc. Chem. Res.* **2022**, *55*, 2148-2161. https://doi.org/10.1021/acs.accounts.2c00311

- (19) Brookhart, M.; Grant, B.; Volpe, A. F., $[(3,5-(CF_3)_2C_6H_3)_4B]^-[H(OEt_2)_2]^+$: a convenient reagent for generation and stabilization of cationic, highly electrophilic organometallic complexes *Organometallics* **1992**, 11, 3920-3922. http://dx.doi.org/10.1021/om00059a071
- (20) Parihar, A.; Emge, T. J.; Chakravartula, S. V. S.; Goldman, A. S., Pincer-Ligated Iridium Complexes with Low-Field Ancillary Ligands: Complexes of (^{iPr}PCP)IrCl₂ and Comparison with (^{iPr}PCP)IrHCl *Organometallics* **2024**, *43*, 1317-1327. https://doi.org/10.1021/acs.organomet.4c00162
- (21) Yang, J.; White, P. S.; Schauer, C. K.; Brookhart, M., Structural and spectroscopic characterization of an unprecedented cationic transition-metal η^1 -silane complex *Angew. Chem., Intl. Ed.* **2008**, *47*, 4141-4143.
- (22) Yang, J.; White, P. S.; Brookhart, M., Scope and Mechanism of the Iridium-Catalyzed Cleavage of Alkyl Ethers with Triethylsilane *J. Am. Chem. Soc.* **2008**, *130*, 17509-17518. https://doi.org/10.1021/ja806419h
- (23) Yang, J.; Brookhart, M., Reduction of alkyl halides by triethylsilane based on a cationic iridium bis(phosphinite) pincer catalyst: scope, selectivity and mechanism *Adv. Synth. Catal.* **2009**, *351*, 175-187.
- (24) Park, S.; Brookhart, M., Hydrosilylation of Carbonyl-Containing Substrates Catalyzed by an Electrophilic h1-Silane Iridium(III) Complex *Organometallics* **2010**, *29*, 6057-6064. https://doi.org/10.1021/om100818y
- (25) Findlater, M.; Cartwright-Sykes, A.; White, P. S.; Schauer, C. K.; Brookhart, M., Role of Coordination Geometry in Dictating the Barrier to Hydride Migration in d⁶ Square-Pyramidal Iridium and Rhodium Pincer Complexes *J. Am. Chem. Soc.* **2011**, *133*, 12274-12284. https://doi.org/10.1021/ja204851x
- (26) Findlater, M.; Schultz, K. M.; Bernskoetter, W. H.; Cartwright-Sykes, A.; Heinekey, D. M.; Brookhart, M., Dihydrogen Complexes of Iridium and Rhodium *Inorg. Chem.* **2012**, *51*, 4672-4678. https://doi.org/10.1021/ic202630x
- (27) Park, S.; Bezier, D.; Brookhart, M., An Efficient Iridium Catalyst for Reduction of Carbon Dioxide to Methane with Trialkylsilanes *J. Am. Chem. Soc.* **2012**, *134*, 11404-11407. https://doi.org/10.1021/ja305318c (28) Haller, L. J.; Mas-Marza, E.; Cybulski, M. K.; Sanguramath, R. A.; Macgregor, S. A.; Mahon, M. F.; Raynaud, C.; Russell, C. A.; Whittlesey, M. K., Computation provides chemical insight into the diverse hydride NMR chemical shifts of [Ru(NHC)₄(L)H](0/+) species (NHC = N-heterocyclic carbene; L = vacant, H₂, N₂, CO, MeCN, O₂, P₄, SO₂, H(-), F(-) and Cl(-)) and their [Ru(R₂PCH₂CH₂PR₂)₂(L)H](+) congeners *Dalton Trans.* **2017**, *46*, 2861-2873. https://doi.org/10.1039/c7dt00117g
- (29) Gordon, B. M.; Parihar, A.; Hasanayn, F.; Goldman, A. S., High Activity and Selectivity for Catalytic Alkane–Alkene Transfer (De)hydrogenation by (^{tBu}PPP)Ir and the Importance of Choice of a Sacrificial Hydrogen Acceptor *Organometallics* **2022**, *41*, 3426–3434. https://doi.org/10.1021/acs.organomet.2c00401
- (30) Gordon, B. M.; Lease, N.; Emge, T. J.; Hasanayn, F.; Goldman, A. S., Reactivity of Iridium Complexes of a Triphosphorus-Pincer Ligand Based on a Secondary Phosphine. Catalytic Alkane Dehydrogenation and the Origin of Extremely High Activity *J. Am. Chem. Soc.* **2022**, *144*, 4133-4146.

https://doi.org/10.1021/jacs.1c13309

- (31) Punji, B.; Emge, T. J.; Goldman, A. S., A Highly Stable Adamantyl-Substituted Pincer-Ligated Iridium Catalyst for Alkane Dehydrogenation *Organometallics* **2010**, *29*, 2702-2709. http://dx.doi.org/10.1021/om100145q
- (32) Krogh-Jespersen, K.; Czerw, M.; Summa, N.; Renkema, K. B.; Achord, P. D.; Goldman, A. S., On the Mechanism of (PCP)Ir-Catalyzed Acceptorless Dehydrogenation of Alkanes: A Combined Computational and Experimental Study *J. Am. Chem. Soc.* **2002**, *124*, 11404-11416. https://doi.org/10.1021/ja012460d
- (33) Kumar, A.; Zhou, T.; Emge, T. J.; Mironov, O.; Saxton, R. J.; Krogh-Jespersen, K.; Goldman, A. S., Dehydrogenation of n-Alkanes by Solid-Phase Molecular Pincer-Iridium Catalysts. High Yields of α -Olefin Product J. Am. Chem. Soc. **2015**, 137, 9894-9911. http://doi.org/10.1021/jacs.5b05313
- (34) Yao, W.; Zhang, Y.; Jia, X.; Huang, Z., Selective Catalytic Transfer Dehydrogenation of Alkanes and Heterocycles by an Iridium Pincer Complex *Angew. Chem., Intl. Ed.* **2014,** *53*, 1390-1394. https://doi.org/10.1002/anie.201306559

(35) Wang, Y.; Qian, L.; Huang, Z.; Liu, G.; Huang, Z., NCP-Type Pincer Iridium Complexes Catalyzed Transfer-Dehydrogenation of Alkanes and Heterocycles *Chin. J. Chem.* **2020**, *38*, 837-841. https://doi.org/10.1002/cjoc.202000097

- (36) Simmons, E. M.; Hartwig, J. F., On the Interpretation of Deuterium Kinetic Isotope Effects in C-H Bond Functionalizations by Transition-Metal Complexes *Angew. Chem., Intl. Ed.* **2012**, *51*, 3066-3072.
- (37) Eisenstein, O.; Crabtree, R. H., Functionalization vs. .beta.-elimination in alkane activation: a key role for 16-electron ML5 intermediates *New Journal of Chemistry* **2001**, *25*, 665-666. https://doi.org/10.1039/b101336j
- (38) Findlater, M.; Choi, J.; Goldman, A. S.; Brookhart, M., Alkane dehydrogenation. In *Catal. Met. Complexes*, Springer: 2012; Vol. 38, pp 113-141.
- (39) Fulmer, G. R.; Miller, A. J. M.; Sherden, N. H.; Gottlieb, H. E.; Nudelman, A.; Stoltz, B. M.; Bercaw, J. E.; Goldberg, K. I., NMR Chemical Shifts of Trace Impurities: Common Laboratory Solvents, Organics, and Gases in Deuterated Solvents Relevant to the Organometallic Chemist *Organometallics* **2010**, *29*, 2176-2179.
- (40) Janowicz, A. H.; Periana, R. A.; Buchanan, J. M.; Kovac, C. A.; Stryker, J. M.; Wax, M. J.; Bergman, R. G., Oxidative Addition of Soluble Ir and Rh Complexes to C-H bonds in Methane and Higher Alkanes *Pure and Appl. Chem.* **1984**, *56*, 13-23.
- (41) Bergman, R. G., Activation of Alkanes with Organotransition Metal Complexes *Science* **1984**, *223*, 902-908.
- (42) Jones, W. D.; Feher, F. J., The mechanism and thermodynamics of alkane and arene carbon-hydrogen bond activation in (C₅Me₅)Rh(PMe₃)(R)H *J. Am. Chem. Soc.* **1984**, *106*, 1650-1653. https://doi.org/10.1021/ja00318a018
- (43) Jones, W. D.; Feher, F. J., Kinetics and thermodynamics of intra- and intermolecular carbon-hydrogen bond activation *J. Am. Chem. Soc.* **1985**, *107*, 620-631. https://pubs.acs.org/doi/pdf/10.1021/ja00289a014 (44) Harper, T. G. P.; Shinomoto, R. S.; Deming, M. A.; Flood, T. C., Activation of Methane by the Reactive Intermediate tris(trimethylphosphine)osmium(0) *J. Am. Chem. Soc.* **1988**, *110*, 7915-7916. doi/10.1021/ja00231a074
- (45) Bennett, J. L.; Vaid, T. P.; Wolczanski, P. T., Extracting absolute titanium-alkyl and -hydride bond enthalpies from relative D(TiR(H)) in (silox)₂(tBu₃SiNH)TiR: electronegativity and ECT models *Inorg. Chim. Acta* **1998**, *270*, 414-423. https://doi.org/10.1016/S0020-1693(97)05997-5
- (46) Wick, D. D.; Jones, W. D., Energetics of Homogeneous Intermolecular Vinyl and Allyl Carbon-Hydrogen Bond Activation by the 16-Electron Coordinatively Unsaturated Organometallic Fragment [Tp'Rh(CNCH2CMe3)] *Organometallics* **1999**, *18*, 495-505. https://doi.org/10.1021/om9808211
- (47) McNamara, B. K.; Yeston, J. S.; Bergman, R. G.; Moore, C. B., The Effect of Alkane Structure on Rates of Photoinduced C-H Bond Activation by Cp*Rh(CO)2 in Liquid Rare Gas Media: An Infrared Flash Kinetics Study *J. Am. Chem. Soc.* **1999**, *121*, 6437-6443.
- (48) Labinger, J. A.; Bercaw, J. E., Understanding and Exploiting C-H Bond Activation *Nature* **2002**, *417*, 507-514. https://www.nature.com/articles/417507a
- (49) Vetter, A. J.; Flaschenriem, C.; Jones, W. D., Alkane Coordination Selectivity in Hydrocarbon Activation by [Tp'Rh(CNneopentyl)]: The Role of Alkane Complexes *J. Am. Chem. Soc.* **2005**, *127*, 12315-12322. https://doi.org/10.1021/ja042152q
- (50) Balcells, D.; Clot, E.; Eisenstein, O., C-H Bond Activation in Transition Metal Species from a Computational Perspective *Chem. Rev.* **2010**, *110*, 749-823. https://doi.org/10.1021/cr900315k
- (51) Hartwig, J. F., Regioselectivity of the Borylation of Alkanes and Arenes *Chem. Soc. Rev.* **2011**, *40*, 1992-2002. https://doi.org/10.1039/C0CS00156B
- (52) Pitts, A. L.; Wriglesworth, A.; Sun, X.-Z.; Calladine, J. A.; Zarić, S. D.; George, M. W.; Hall, M. B., Carbon–Hydrogen Activation of Cycloalkanes by Cyclopentadienylcarbonylrhodium—A Lifetime Enigma *J. Am. Chem. Soc.* **2014**, *136*, 8614-8625. https://doi.org/10.1021/ja5014773
- (53) Zhao, Y.; Truhlar, D. G., A new local density functional for main-group thermochemistry, transition metal bonding, thermochemical kinetics, and noncovalent interactions *J. Chem. Phys.* **2006**, *125*, 194101/194101-194101/194118. https://doi.org/10.1063/1.2370993

- (54) Frisch, M. J.; Trucks, G. W., et al. Gaussian 16, Revision D.01, Gaussian, Inc.: Wallingford CT., 2016.
- (55) Krishnan, R.; Binkley, J. S.; Seeger, R.; Pople, J. A., Self-consistent molecular orbital methods. XX. A basis set for correlated wave functions *J. Chem. Phys.* **1980**, *72*, 650-654. https://doi.org/10.1063/1.438955
- (56) Andrae, D.; Haeussermann, U.; Dolg, M.; Stoll, H.; Preuss, H., Energy-adjusted ab initio pseudopotentials for the second and third row transition elements *Theor. Chim. Acta* **1990**, *77*, 123-141. https://doi.org/10.1007/BF01114537
- (57) Ehlers, A. W.; Böhme, M.; Dapprich, S.; Gobbi, A.; Höllwarth, A.; Jonas, V.; Köhler, K. F.; Stegmann, R.; Veldkamp, A.; Frenking, G., A set of f-polarization functions for pseudo-potential basis sets of the transition metals Sc–Cu, Y–Ag and La–Au *Chem. Phys. Lett.* **1993**, *208*, 111-114. https://doi.org/10.1016/0009-2614(93)80086-5
- (58) Marenich, A. V.; Cramer, C. J.; Truhlar, D. G., Universal Solvation Model Based on Solute Electron Density and on a Continuum Model of the Solvent Defined by the Bulk Dielectric Constant and Atomic Surface Tensions *J. Phys. Chem. B* **2009**, *113*, 6378-6396. https://doi.org/10.1021/jp810292n
- (59) Chai, J.-D.; Head-Gordon, M., Long-range corrected hybrid density functionals with damped atom—atom dispersion corrections *Phys. Chem. Chem. Phys.* **2008**, *10*, 6615-6620. http://dx.doi.org/10.1039/B810189B
- (60) Lee, C.; Yang, W.; Parr, R. G., Development of the Colle-Salvetti correlation-energy formula into a functional of the electron density *Phys. Rev. B* **1988**, *37*, 785-789. https://doi.org/10.1103/PhysRevB.37.785
- (61) Adamo, C.; Barone, V., Toward reliable density functional methods without adjustable parameters: The PBE0 model *J. Chem. Phys.* **1999**, *110*, 6158-6170. https://doi.org/10.1063/1.478522
- (62) Grimme, S.; Antony, J.; Ehrlich, S.; Krieg, H., A consistent and accurate ab initio parametrization of density functional dispersion correction (DFT-D) for the 94 elements H-Pu J. Chem. Phys. **2010**, 132, 154104. https://doi.org/10.1063/1.3382344
- (63) Weigend, F.; Ahlrichs, R., Balanced basis sets of split valence, triple zeta valence and quadruple zeta valence quality for H to Rn: Design and assessment of accuracy *Phys. Chem. Chem. Phys.* **2005**, *7*, 3297-3305. http://dx.doi.org/10.1039/B508541A
- (64) Weigend, F., Accurate Coulomb-fitting basis sets for H to Rn *Phys. Chem. Chem. Phys.* **2006**, *8*, 1057-1065. http://dx.doi.org/10.1039/B515623H
- (65) Ochterski, J. W. Thermochemistry in Gaussian; page 13. https://gaussian.com/thermo/ accessed January 2024.
- (66) Cramer, C. J., Essentials of Computational Chemistry: Theories and Models, 2nd Edition Wiley: 2004.
- (67) Wertz, D. H., Relationship between the gas-phase entropies of molecules and their entropies of solvation in water and 1-octanol *J. Am. Chem. Soc.* **1980,** *102*, 5316-5322. https://doi.org/10.1021/ja00536a033
- (68) Brookhart, M.; Green, M. L. H.; Parkin, G., Agostic Interactions in Transition Metal Compounds *Proc. Natl. Acad. Sci.* **2007**, *104*, 6908-6914. https://doi.org/10.1073/pnas.0610747104
- (69) Barakat, M.; Elhajj, S.; Yazji, R.; Miller, A. J. M.; Hasanayn, F., Kinetic Isotope Effects and the Mechanism of CO₂ Insertion into the Metal-Hydride Bond of fac-(bpy)Re(CO)₃H *Inorg. Chem.* **2024**, https://doi.org/10.1021/acs.inorgchem.4c01246
- (70) Fan, Y.; Cui, X.; Burgess, K.; Hall, M. B., Electronic Effects Steer the Mechanism of Asymmetric Hydrogenations of Unfunctionalized Aryl-Substituted Alkenes *J. Am. Chem. Soc.* **2004**, *126*, 16688-16689. http://dx.doi.org/10.1021/ja044240g
- (71) Mendelsohn, L. N.; Pavlovic, L.; Zhong, H.; Friedfeld, M. R.; Shevlin, M.; Hopmann, K. H.; Chirik, P. J., Mechanistic Investigations of the Asymmetric Hydrogenation of Enamides with Neutral Bis(phosphine) Cobalt Precatalysts *J. Am. Chem. Soc.* **2022**, *144*, 15764-15778. https://doi.org/10.1021/jacs.2c06454
- (72) Biosca, M.; de la Cruz-Sánchez, P.; Faiges, J.; Margalef, J.; Salomó, E.; Riera, A.; Verdaguer, X.; Ferré, J.; Maseras, F.; Besora, M.; Pàmies, O.; Diéguez, M., P-Stereogenic Ir-MaxPHOX: A Step toward Privileged Catalysts for Asymmetric Hydrogenation of Nonchelating Olefins *ACS Catal.* **2023**, *13*, 3020-3035. https://doi.org/10.1021/acscatal.2c05579
- (73) Oxgaard, J.; Periana, R. A.; Goddard, W. A., III, Mechanistic Analysis of Hydroarylation Catalysts *J. Am. Chem. Soc.* **2004**, *126*, 11658-11665. https://doi.org/10.1021/ja048841j

(74) Oxgaard, J.; Muller, R. P.; Goddard, W. A.; Periana, R. A., Mechanism of Homogeneous Ir(III) Catalyzed Regioselective Arylation of Olefins *J. Am. Chem. Soc.* **2004**, *126*, 352-363. https://doi.org/10.1021/ja034126i (75) Bellows, S. M.; Cundari, T. R.; Jones, W. D., Methane Is the Best Substrate for C(sp³)—H Activation with Cp*(PMe³)Co(Me)(OTf): A Density Functional Theory Study *Organometallics* **2015**, *34*, 4032-4038. http://dx.doi.org/10.1021/acs.organomet.5b00452

- (76) Perutz, R. N.; Sabo-Etienne, S., The σ-CAM Mechanism: σ Complexes as the Basis of σ-Bond Metathesis at Late-Transition-Metal Centers *Angew. Chem., Intl. Ed.* **2007**, *46*, 2578-2592. http://dx.doi.org/10.1002/anie.200603224
- (77) Perutz, R. N.; Sabo-Etienne, S.; Weller, A. S., Metathesis by Partner Interchange in σ -Bond Ligands: Expanding Applications of the σ -CAM Mechanism *Angew. Chem., Intl. Ed.* **2022,** *61*, e202111462. https://doi.org/10.1002/anie.202111462
- (78) Carlsen, R.; Maley, S. M.; Ess, D. H., Timing and Structures of σ-Bond Metathesis C-H Activation Reactions from Quasiclassical Direct Dynamics Simulations *Organometallics* **2021**, *40*, 1454-1465. https://doi.org/10.1021/acs.organomet.1c00102
- (79) Ess, D. H., Quasiclassical Direct Dynamics Trajectory Simulations of Organometallic Reactions *Acc. Chem. Res.* **2021**, *54*, 4410-4422. https://doi.org/10.1021/acs.accounts.1c00575
- (80) β-H-transfer before H-H reductive bond formation, to give the Ir(V) species **1-(H)**₂(alkene)(H)⁺, is also possible in principle but barriers to this reaction are calculated to be extremely high.